

## Machine learning techniques and multi-scale models to evaluate the impact of silicon dioxide ( $\text{SiO}_2$ ) and calcium oxide (CaO) in fly ash on the compressive strength of green concrete

Dilshad Kakasor Ismael Jaf<sup>a,\*</sup>, Payam Ismael Abdulrahman<sup>b</sup>, Ahmed Salih Mohammed<sup>c,d</sup>, Rawaz Kurda<sup>e</sup>, Shaker M.A. Qaidi<sup>f</sup>, Panagiotis G. Asteris<sup>g,\*</sup>

<sup>a</sup> Civil Engineering Department, College of Engineering, Salahaddin University-Erbil, Kurdistan, Iraq

<sup>b</sup> Civil Engineering Department, College of Engineering, Tishk International University-Erbil, Erbil, Kurdistan Region, Iraq

<sup>c</sup> Civil Engineering Department, College of Engineering, University of Sulaimani, Kurdistan, Iraq

<sup>d</sup> The American University of Iraq, Sulaimani (AUIS), Sulaimani, Kurdistan Region, Iraq

<sup>e</sup> Department of Highway and Bridge Engineering, Technical Engineering College, Erbil Polytechnic University, Erbil 44001, Iraq

<sup>f</sup> Department of Civil Engineering, College of Engineering, University of Duhok, Duhok, Kurdistan-Region, Iraq

<sup>g</sup> Computational Mechanics Laboratory, School of Pedagogical and Technological Education, Athens, Greece

### ARTICLE INFO

#### Keywords:

Artificial neural network  
Concrete  
CaO (%)  
 $\text{SiO}_2$  (%)  
Fly Ash  
Soft Computing

### ABSTRACT

Fly ash is a by-product almost found in coal power plants; it is available worldwide. According to the hazardous impacts of cement on the environment, fly ash is known to be a suitable replacement for cement in concrete. A lot of carbon dioxide ( $\text{CO}_2$ ) is released during cement manufacturing. The investigations estimate that about 8–10% of the total  $\text{CO}_2$  emissions are maintained by cement production. Since fly ash has nearly the same chemical compounds as cement, it can be utilized as a suitable alternative to cement in concrete (green concrete). The current study analyzes the effect of the quantity of the two main components of fly ash, CaO, and  $\text{SiO}_2$ , on the compressive strength of concrete modified with different fly ash content for various mix proportions. For this purpose, various concrete samples modified with fly ash were collected from the literature (236 datasets), analyzed, and modeled using four different models; Full-quadratic (FQ), Nonlinear regression (NLR), Multi-linear regression (MLR), and Artificial neural network (ANN) model to predict the compressive strength of concrete with different geometry and size of the specimens. The accuracy of the models was evaluated using correlation coefficient ( $R^2$ ), Mean absolute error (MAE), Root mean squared error (RMSE), Scatter Index (SI), a-20 index, and Objective function (OBJ). According to the modeling results, increasing  $\text{SiO}_2$  (%) increased the compressive strength, while increasing CaO (%) increased compressive strength only when the cement replacement with fly ash was between 52 and -100%. Based on  $R^2$ , RMSE, and MAE, the ANN model was the most effective and accurate on predicting the compressive strength of concrete in different strength ranges. According to the sensitivity analysis, curing time is the most critical characteristic for predicting the compression strength of concrete using this database. The primary objective of this work is to explore and evaluate various machine-learning models for predicting compressive resistance. The study emphasizes these models' development, comparison, and performance assessment, highlighting their potential to predict compressive strength accurately. The research primarily uses machine learning, leveraging algorithms and techniques to build predictive models. The focus is on harnessing the power of data-driven approaches to improve the accuracy and reliability of compressive strength predictions.

### 1. Introduction

Cement production provides 8 to 10 % of the  $\text{CO}_2$  emissions in the

world [1]. Cement is an important factor that leads to greenhouse gases and global warming [2]. The key variables that lead to social and economic changes are industrialization, urbanization, globalization of the

\* Corresponding authors.

E-mail addresses: [dilshad.jaf@su.edu.krd](mailto:dilshad.jaf@su.edu.krd) (D. Kakasor Ismael Jaf), [payam.ismael@alm.tiu.edu.iq](mailto:payam.ismael@alm.tiu.edu.iq) (P. Ismael Abdulrahman), [ahmed.mohammed@univsul.edu.iq](mailto:ahmed.mohammed@univsul.edu.iq) (A. Salih Mohammed), [rawaz.kurda@epu.edu.iq](mailto:rawaz.kurda@epu.edu.iq) (R. Kurda), [shaker.abdal@uod.ac](mailto:shaker.abdal@uod.ac) (S.M.A. Qaidi), [asteris@aspete.gr](mailto:asteris@aspete.gr) (P.G. Asteris).

economy, market and consumerism, and population increase. Overall, climate change is a clear result of these factors resulting in dangerous issues for humanity [3]. The rapid development of globalization and population growth has caused an increase in building construction [4]. The construction business is growing exponentially, resulting in an increasing demand for construction materials, especially cement [5]. Nowadays, the construction industry is one of the largest environmental impacts among all human activities [6]. The negative environmental impacts associated with the widespread use of cement have encouraged researchers to find a satisfactory solution for reducing the demand for cement. As the greatest strategy to reduce CO<sub>2</sub> emissions is to replace cement with a suitable substitute in percentage, several studies have been done to find viable replacements for cement in concrete mixtures. Supplementary cementitious materials (SCMs) like fly ash [7], silica fume [8], ground granulated blast furnace slag [9], rice husk ash [10], and metakaolin [11] can be added to the concrete as a partial replacement. Fly ash is a widely available material worldwide [12]. It is a very fine powder with a fineness more than cement. Fly ash is commonly a by-product material found in coal industries and collected in a baghouse or on an electrostatic precipitator. Fly ash is one of the best alternatives for cement in concrete; it provides excellent mechanical properties [13]. Utilizing fly ash in concrete economizes the mix, protects the environment from disposal, conserves more land, and reduces cement production; overall, it can improve the properties of green and hardened concrete [14–16].

Fly ash is a pozzolanic material rich in aluminous and siliceous substances. Generally, the chemical compositions and their ratios are source-dependent. According to the ASTM C619 [17], fly ash is divided into two classes based on the quantity of chemical compositions; class C and F [18,19]. Both classes of fly ash can be added to concrete in a specific range to enhance mechanical properties and durability. Numerous studies have been conducted on cement-based concrete modified with different types, classes, and quantities of fly ash. The improvement greatly depends upon the type and ratio of fly ash. The fly ash type correspondence to the number of chemical substances and their impact on the concrete properties. Among the chemical compositions of fly ash, the effect of various silicon dioxide (SiO<sub>2</sub>) and calcium oxide (CaO) ratios on the mechanical properties of concrete has been investigated in previous studies. Class C of fly ash provides a greater compressive strength value for the same cement dosage and fly ash percentage than class F [19]. Fly ash with a higher CaO content tends to have a higher reactivity [20]. The fly ash compounds such as CaO at early ages and SiO<sub>2</sub> at later ages are associated with the strength gain of concrete [21].

Compressive strength is a significant mechanical property in concrete considered in all concrete structure works. Concrete is a heterogeneous material comprising different substances, such as cement, aggregate, water, and admixtures, resulting in different compressive strength values [22]. All the physical, chemical and mechanical characteristics of these ingredients and their quantity impact the compressive loading capacity of concrete [23]. The compressive strength value is achieved in the laboratory during the testing of the concrete samples by crushing the cylinders or cubes of standard dimension [24]. The experimental method is standardized all over the world. However, nowadays, laboratory tests are inefficient and uneconomical since it is costly and time-consuming. Recently, with the advancement of Artificial Intelligence (AI), Machine learning algorithm (ML), has been applied to predict several mechanical properties in concrete [25]. ML techniques such as regression, clustering, and classification can estimate various factors with varying efficiency and accurately forecast concrete compressive strength value [26]. Modeling the properties of concrete can be developed in various ways, including statistical techniques, computational modeling, and newly created tools like artificial neural networks (ANN), regression analysis, and the M5P-tree model [27–31].

In the current study, 236 experimental values of compressive strength have been collected from the literature. The concrete mixtures included fly ash content (FA) ranging (from 71 – 316 kg/m<sup>3</sup>), CaO (0.31 – 32%), SiO<sub>2</sub> (30.5 – 62.54%), cement content (C) (67 – 356 kg/m<sup>3</sup>), cement replacement (CR) (18 – 100%), coarse aggregate (CA) (801 – 1246 kg/m<sup>3</sup>), fine aggregate (S) (522 – 905 kg/m<sup>3</sup>), water-to-binder ratio (w/b) (0.28 – 0.6), and curing time (t) (3 – 365 days). As well as the compressive strength (CS) ranged from 7.98 to 92.93 MPa. To check the reliability and applicability of the models, CS is divided into three different ranges; 5 to 34 MPa, 35 to 64 MPa, and 65 to 95 MPa. Then the most effective model is applied to those ranges. This study proposes models to predict compressive strength values using different analyzing approaches. The influence of CaO and SiO<sub>2</sub> contents at various mix proportions on the compressive strength of cement-based concrete modified with fly ash was studied and qualified in this study. In the modeling part, full quadratic (FQ), nonlinear (NLR), multi-linear (MLR), and artificial neural network (ANN) models are used to develop predictive models. In addition, different statistical tools such as Correlation coefficient (R<sup>2</sup>), Root mean squared error (RMSE), Mean absolute error (MAE), Scatter index (SI), Objective function (OBJ), and an a20-index are used to evaluate the reliability and accuracy of the developed models.

## 2. Research significant

The following are the general objectives of this study:

- i. Statistically analyzing the collected data and evaluating the effect of CaO and SiO<sub>2</sub> on the compressive strength of fly ash-modified concrete, such as coarse aggregate, fine aggregate, cement, cement replacement, water-to-binder ratio (w/b), fly ash, calcium oxide (CaO,%), silicon dioxide (SiO<sub>2</sub>,%), and curing time.
- ii. Creating an accurate and reliable model for predicting the compressive strength of fly ash-based concrete.
- iii. Conducting sensitivity analysis to determine the most important parameter in predicting the compressive strength of concrete modified with various types and classes of fly ash.

## 3. Methodology

The methodology of the current study includes a series of steps which has been drawn as a flowchart and shown in Fig. 1. The main steps involve the following;

- i. Creating and collecting data on the cement-based concrete in different strength ranges of (5 – 34 MPa), (35 – 64 MPa), and (65 – 95 MPa) from the literature.
- ii. Considering coarse aggregate (CA), fine aggregate (S), cement content (C), fly ash content (FA), cement replacement (CR), water-to-binder ratio (w/b), calcium oxide (CaO), silicon dioxide (SiO<sub>2</sub>), and curing time (t) as predictors for the models whereas, the compressive strength (CS) is considered as a target value of the models.
- iii. Randomly mixing the collected data into two groups, 70% of the data as training and 30% as testing.
- iv. Developing predictive models using Full Quadratic (FQ), Nonlinear Regression (NLR), Multi-linear Regression (MLR), and Artificial Neural Networks (ANN) models.
- v. Evaluating the proposed models based on R<sup>2</sup>, RMSE, MAE, OBJ, SI, and the a-20 index.
- vi. Conducting sensitivity analysis to find the essential parameter in predicting compressive strength for the concrete modified with fly ash.

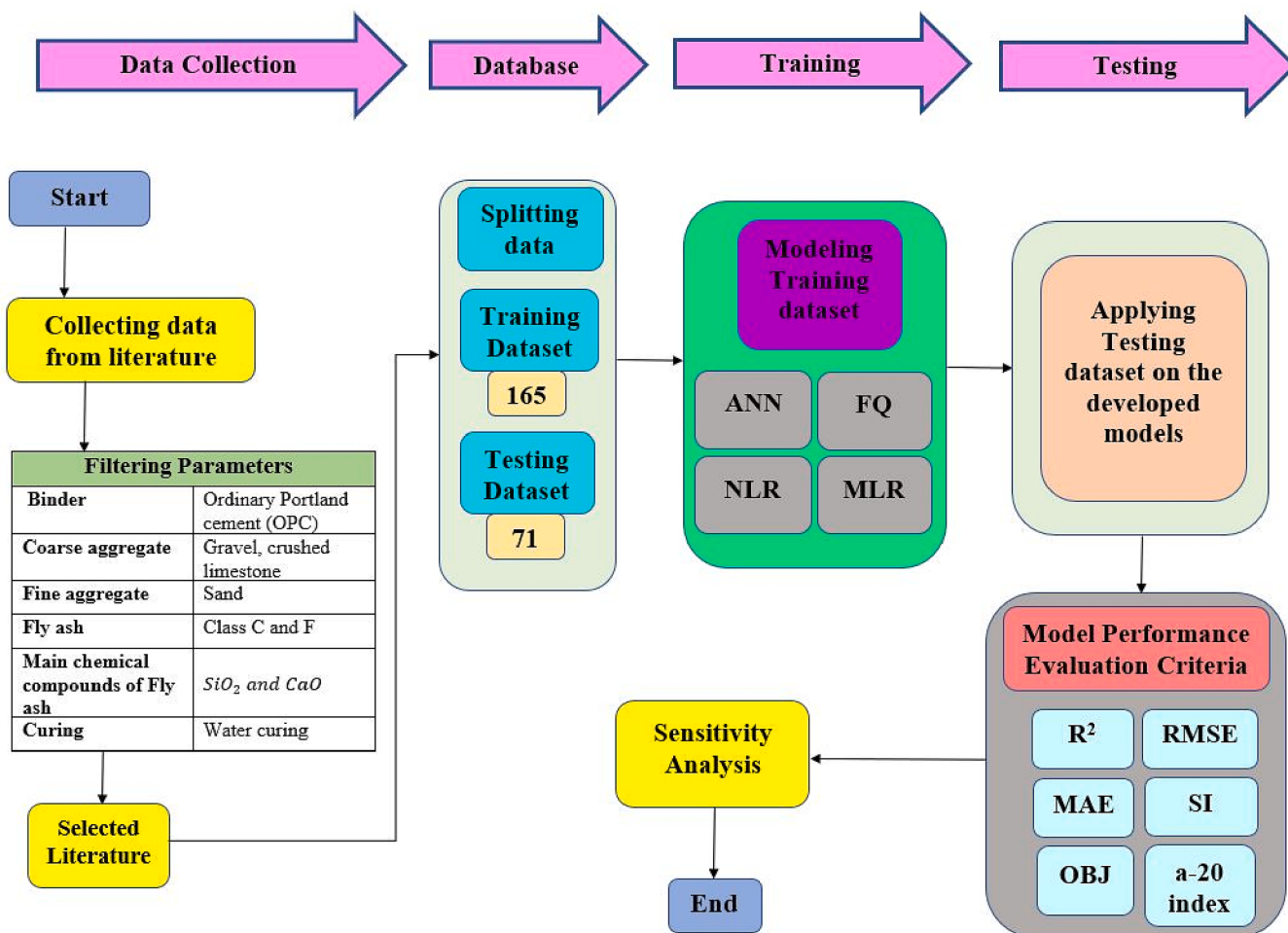


**Fig. 1.** Methodology of Research; ANN, artificial neural network; FQ, full quadratic; NLR, nonlinear; MLR, multi-linear;  $R^2$ , correlation coefficient; RMSE, root mean squared error; MAE, mean absolute error; SI, scatter index; OBJ, objectives.

### 3.1. Data collection

To develop a reliable model to predict the compressive strength of concrete modified with fly ash, 236 data were collected from the literature, including various fly ash ratios with class F and C, resulting in different ratios of main chemical compositions such as;  $CaO$  and  $SiO_2$ . As well as different coarse and fine aggregate content, cement content, and the curing regime was involved. Table 1 shows a summary of the collected data. A total of 236 data were selected in this study, and based on the information from the literature [32–34], the data were divided into two groups using RAND Function.

Training data was included;  $0.70 * \text{No.ofdataset}(236) = 165$  Data.

The training data was used to develop the models.

Tested data;  $0.30 * \text{No.ofdataset}(236) = 71$  Data The testing dataset was used to validate (Check) the developed equations based on 165 datasets.

### 3.2. Pre-processing

Pre-processing is required before using the dataset. Pre-processing techniques improve the performance of computational models. As a result, all discontinuous features (independent variables) were converted to dummy variables using Pandas, an open-source Python package. As demonstrated in the box plot (Fig. 2), some features in the created dataset had values that spanned an exceptionally wide range, which was incompatible with model learning. Therefore, the average of the upper and lower bounds was employed instead. Furthermore, using

the original non-normalized data may have influenced the ML model's performance [35]. This study pre-processed the database by converting each independent variable to a value between zero and one using the following equation, Eq. (1).

$$X_f = \frac{(X_i - X_{i\min})(X_{i\max} - X_{i\min})}{(X_{i\max} - X_{i\min})} + X_{i\min} \quad (1)$$

where;  $X_i$  is the old value and  $X_f$  is the new value. The  $X_{i\min}$  is zero and  $X_{i\max}$  is one.

### 3.3. Statistical analysis

The collected data is statistically analyzed to determine the distribution of each independent variable with the dependent variable (compressive strength). Therefore, statistical parameters such as Mean, Standard Deviation (SD), Variance (Var), Kurtosis (Kur), Skewness (Skew), minimum (Min), and Maximum (Max) are obtained. For kurtosis, the negative value indicated a short distribution tail, while the positive indicated a longer tail. However, skewness shows the distribution of the variable, whether in the right or the left tail, with the right for positive and the left for negative values.

The relation between compressive strength and the mentioned independent variables is plotted in Fig. 3. The compressive strength data is shown in a frequency histogram in Fig. 4. The statistical analysis is summarized in Table 2.

**Table 1**

Summary of collected data for cement-based concrete modified with fly ash.

Reference	No. of Data	Coarse aggregate, CA (kg/m <sup>3</sup> )	Sand, S (kg/m <sup>3</sup> )	Cement, C (kg/m <sup>3</sup> )	Fly ash (kg/m <sup>3</sup> )	Cement replacement, CR (%)	Water-to-binder ratio, (w/b)	CaO (%)	SiO <sub>2</sub> (%)	Curing time, t (Days)	Compressive strength, CS (MPa)
[58]	53	801—1090	687–905	144–356	92–168	35–100	0.41–0.60	2.32	52.1	3, 7, 14, 28, 56 and 91	11.78–45.99
[15]	60	1270	522–671	160–320	80–240	20–60	0.30–0.40	1.54	62.54	7, 28, 56, 90, 180, 256 and 365	16.99–92.93
[59]	42	1016–1207	607–854	107–328	71–316	18–74	0.3–0.4	27.6–31.9	30.5–34.9	3, 7, 28, 90 and 365	15.4–72.4
[60]	13	1089–1124	726–749	179–182	219–222	55	0.3–0.4	0.3–15.8	36.9–56.8	3, 7, 28, 56, and 91	21.2–44.6
[61]	9	843–864	842–866	161–247	155–254	40–60	0.4–0.5	13.4	52.4	7 and 28	15.6–48.3
[62]	23	1200	600	120–200	200–280	50–70	0.3–0.4	2.4–2.6	44.9–50.2	3, 7, 28, 90, 180, and 365	7.98–81.54
[63]	15	1181–1246	600–819	66.9–200	167–280	50–80	0.28–0.40	2.6–26.3	35.2–50.2	7, 14, 28, 90, 180 and 365	16–67.5
[64]	17	1095–1195	740–797	150–274	117–204	30–52	0.4–0.5	4.2–13.4	42.7–52.4	7, 28, 56, and 96	25.5–42.5
[65]	4	1114–1135	727–740	157–238	159–236	40–60	0.3	2.9	52	14 and 28	38–62
Remark	236	Ranged between 801 and 1200	Ranged between 522 and 905	Ranged between 107 and 356	Varied between 71 and 316	Ranged between 18 and 100	Varied between 0.28 and 0.6	Ranged between 0.3 and 31.9	Ranged between 30.5 and 62.54	Ranged between 3 and 365	Ranged between 7.98 and 92.93

### 3.4. Specimen sizes

The specimen parameters such as size and shape are important factors in the compressive strength of concrete. Those factors were investigated in the normal and high-strength concrete in the previous study [36,37]. In the current study, the database utilized to create the models comprised test samples of different sizes and shapes for assessing compressive strength. Standard cylinders with S1 (100 × 200) and S2

(150 × 300) mm, and cubes with S3 (100 × 100 × 100) and S4 (150 × 150 × 150) mm were included.

The samples were all utilized to create predictive models. Using different models, the constructed models were evaluated using various specimen sizes to determine the efficiency of predicted compressive strength. 39% of the data were S1, and 18%, 41%, and 2% were S2, S3, and S4, respectively. The total number for all specimen sizes in the training and testing datasets is shown in Fig. 5.

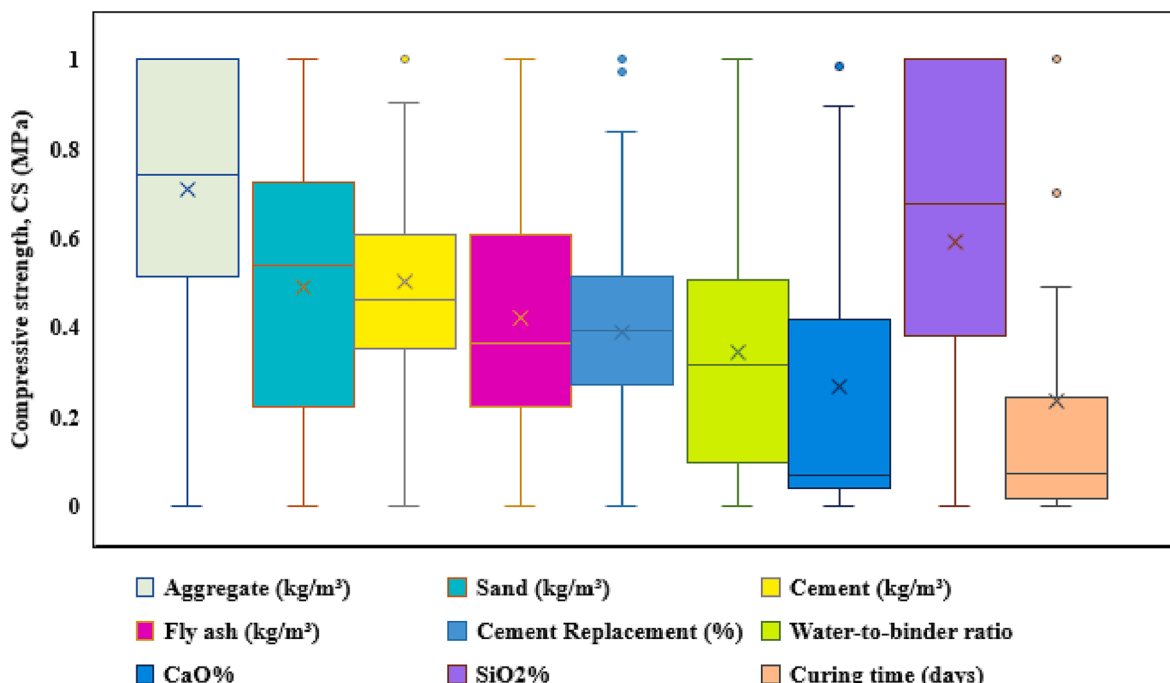
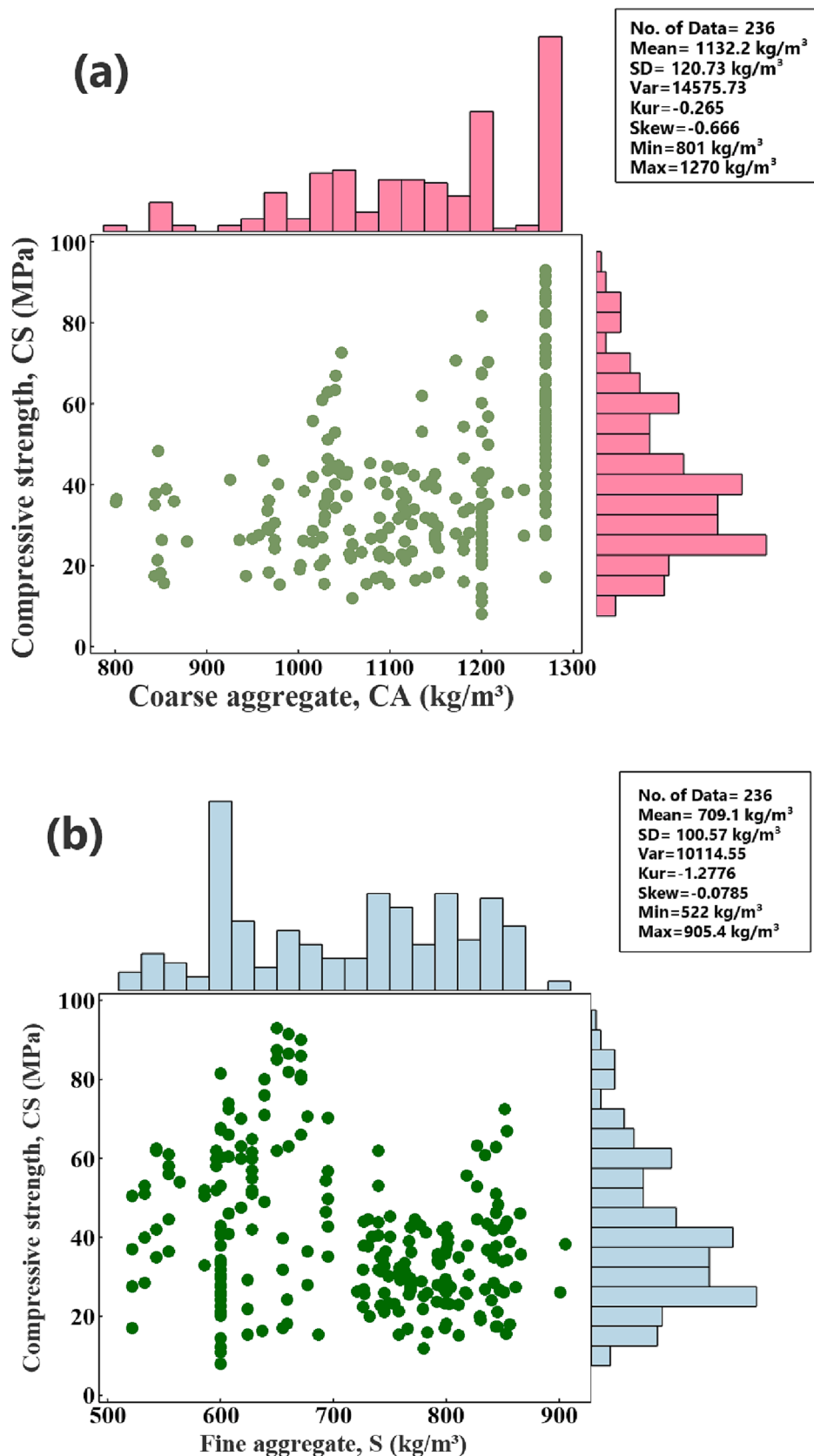


Fig. 2. Box plot of the independent variables.



**Fig. 3.** Marginal plots for the compressive strength of concrete with (a) coarse aggregate ( $\text{kg}/\text{m}^3$ ) (b) fine aggregate ( $\text{kg}/\text{m}^3$ ) (c) cement ( $\text{kg}/\text{m}^3$ ) (d) fly ash ( $\text{kg}/\text{m}^3$ ) (e) cement replacement (%) (f) water-to-binder ratio (g)  $\text{CaO}$  (%) (h)  $\text{SiO}_2$  (%), and (i) curing time (days).

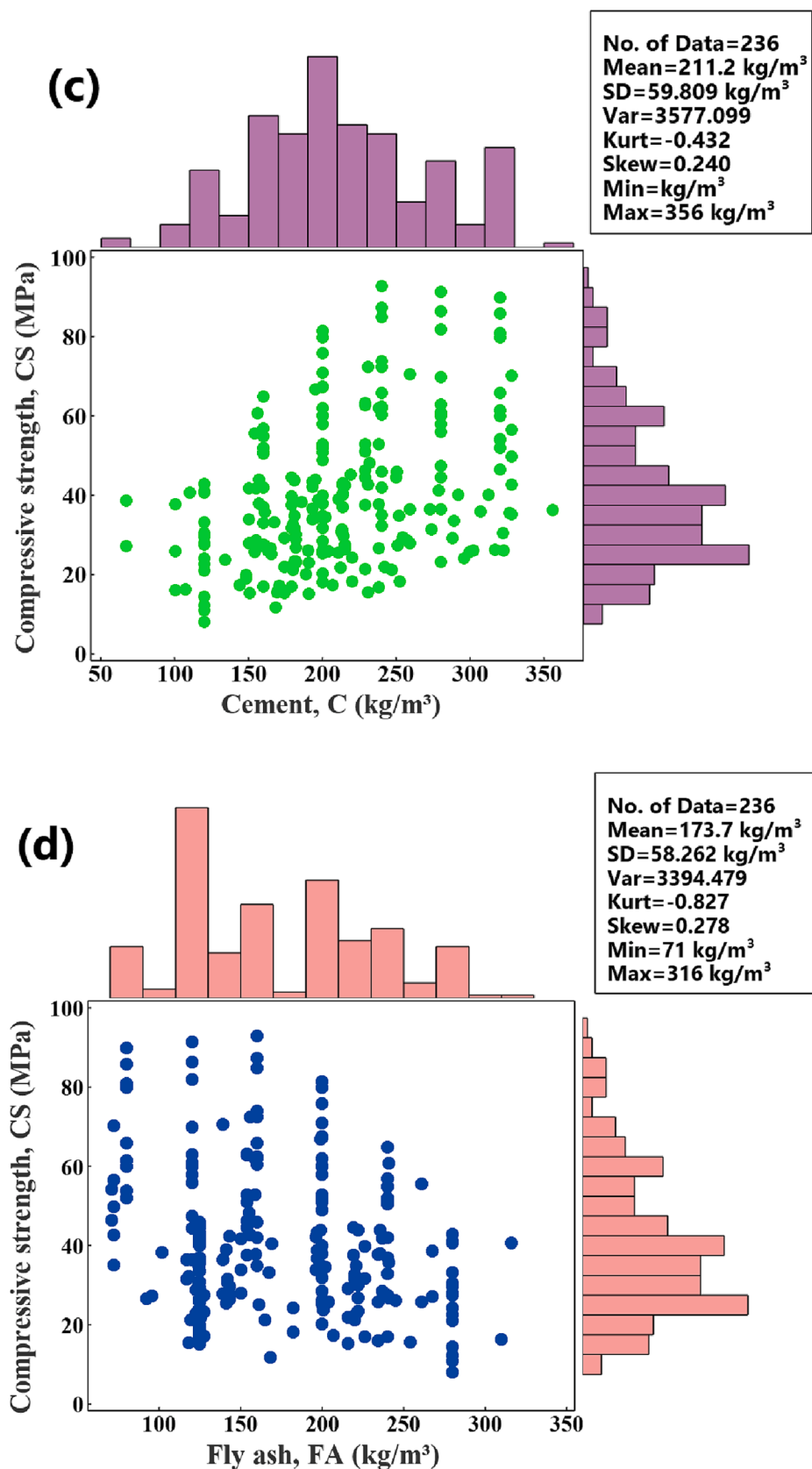


Fig. 3. (continued).

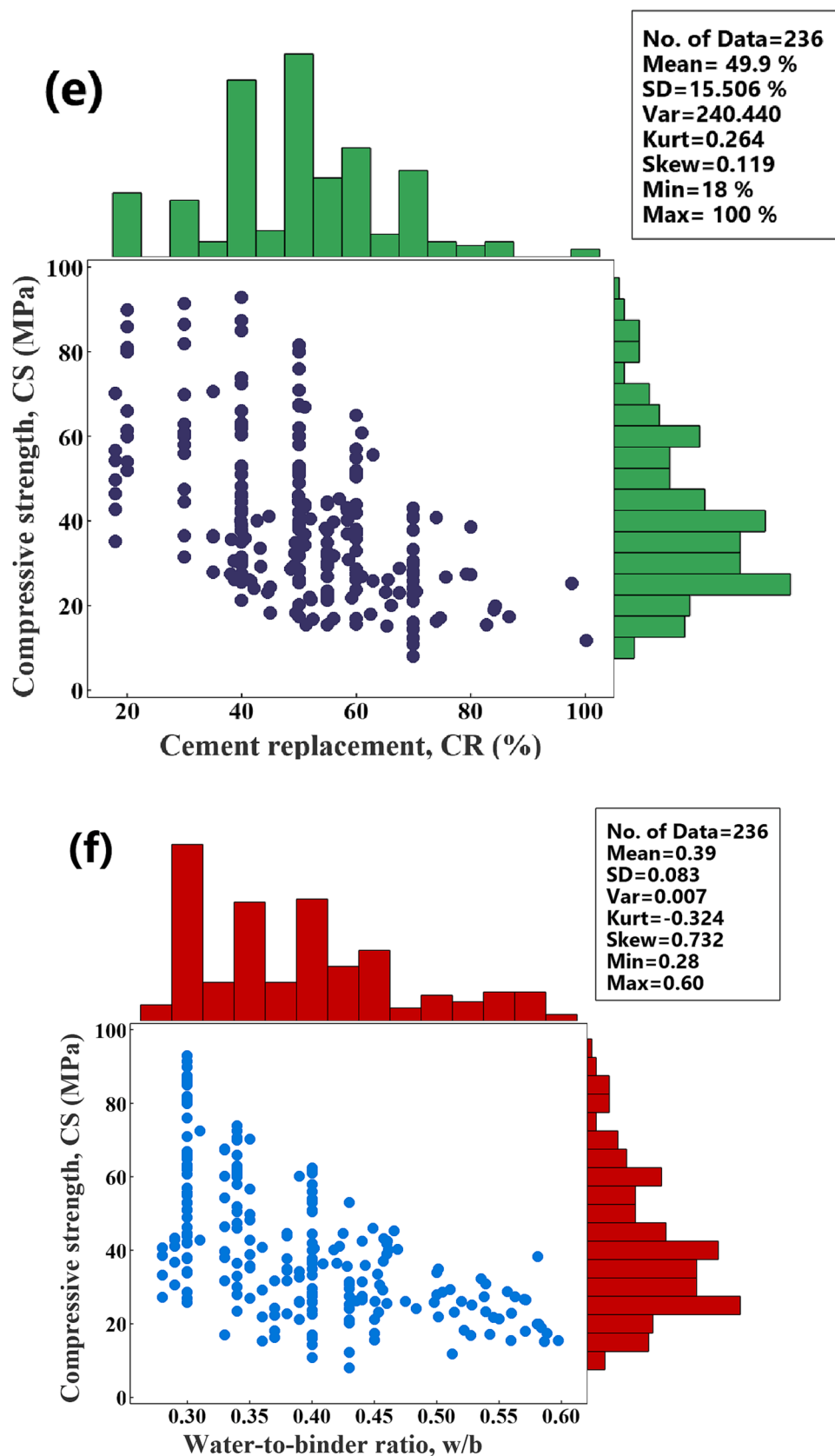


Fig. 3. (continued).

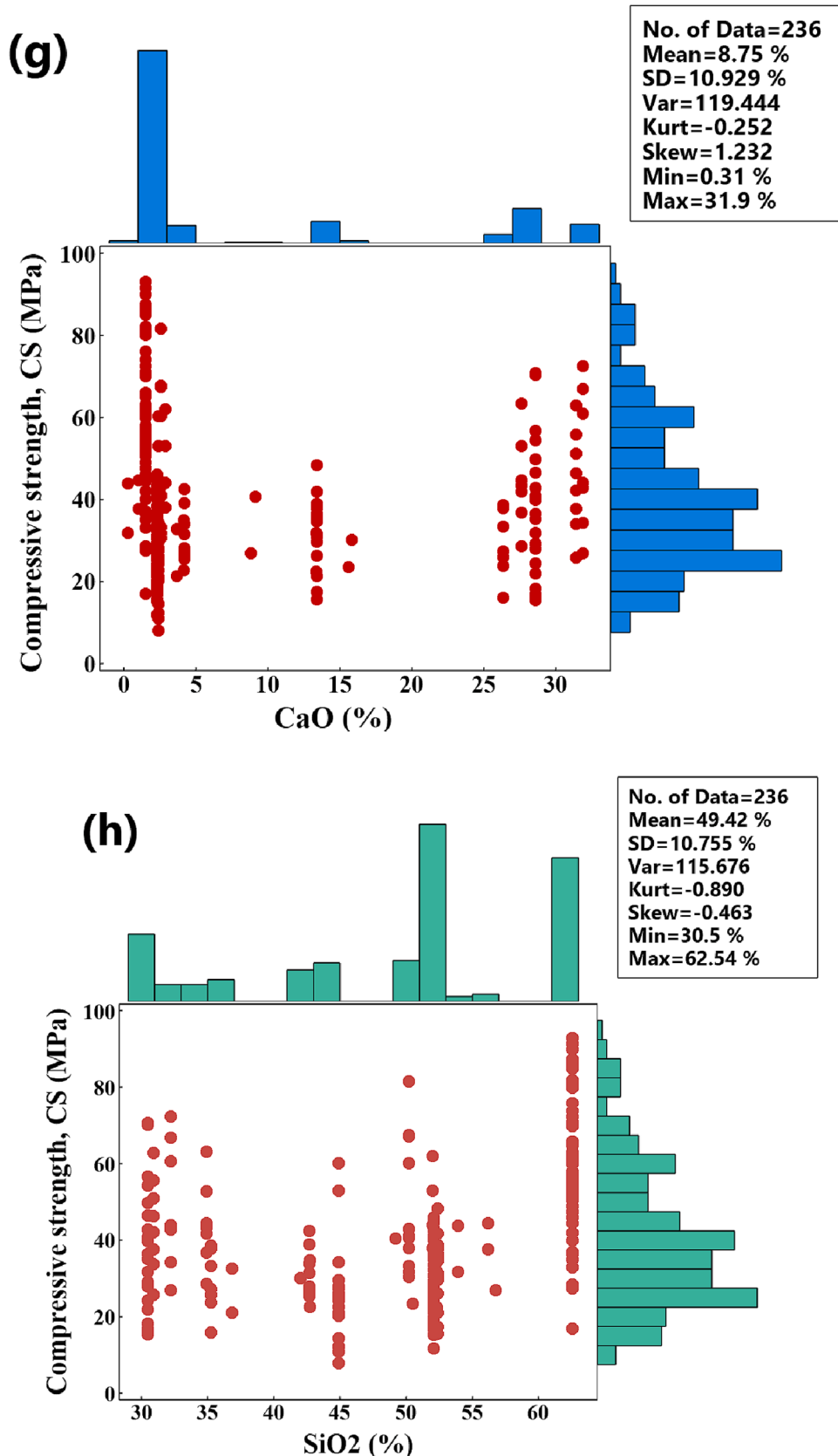


Fig. 3. (continued).

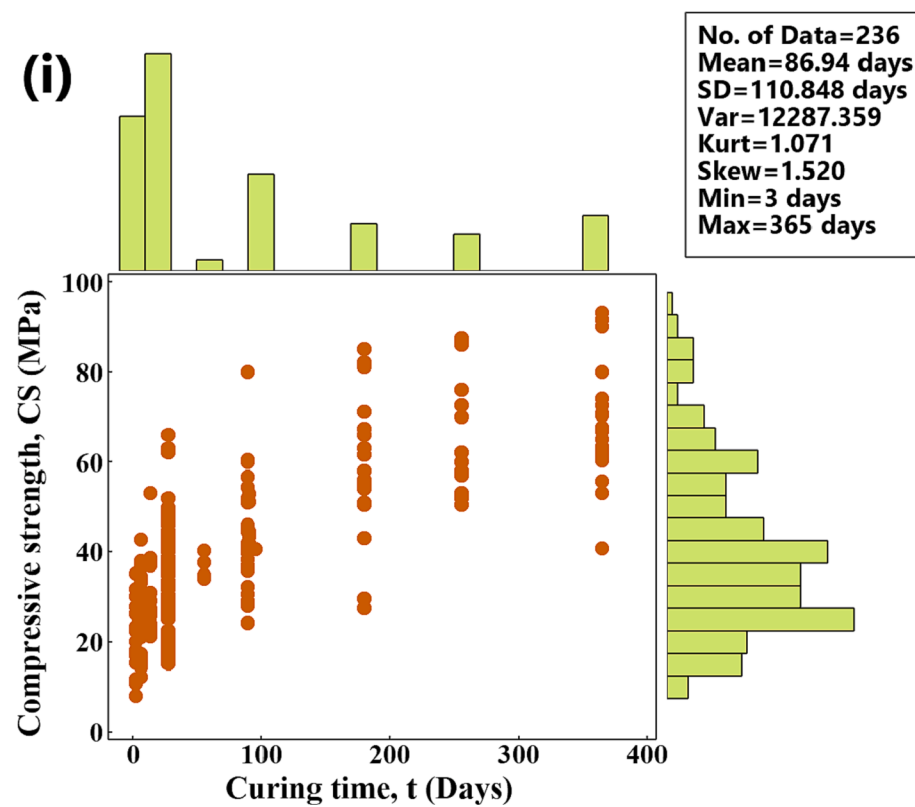


Fig. 3. (continued).

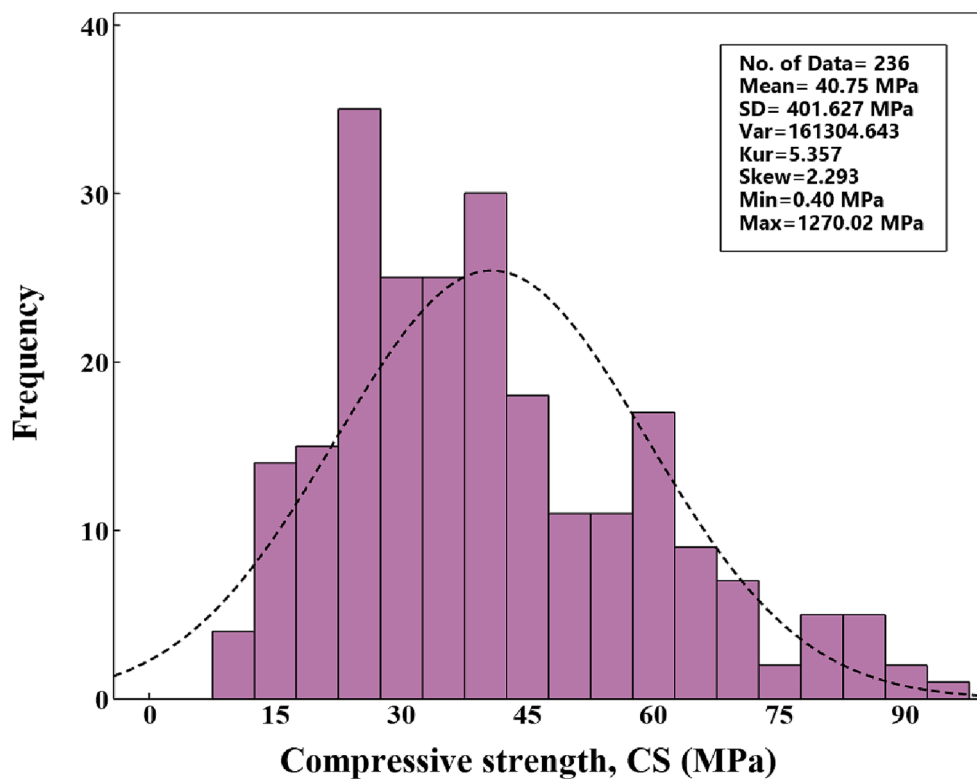


Fig. 4. Histogram for compressive strength (MPa) of concrete modified with fly ash.

**Table 2**

Summary of statistical analysis of the concrete parameters.

Variables	Statistical parameters						
	Mean	Standard deviation	Variance	Kurtosis	Skewness	Min	Max
CA ( $\text{kg}/\text{m}^3$ )	1132.2	120.73	14575.73	-0.265	-0.666	801	1270
S ( $\text{kg}/\text{m}^3$ )	709.1	100.57	10114.55	-1.2776	-0.0785	522	905.4
C ( $\text{kg}/\text{m}^3$ )	211.2	59.809	3577.099	-0.432	0.240	67	356
FA ( $\text{kg}/\text{m}^3$ )	173.7	58.262	3394.479	-0.827	0.278	71	316
CR (%)	49.9	15.506	240.440	0.264	0.119	18	100
w/b	0.39	0.083	0.007	-0.324	0.732	0.28	0.60
CaO (%)	8.75	10.929	119.444	-0.252	1.232	0.31	31.9
SiO <sub>2</sub> (%)	49.42	10.755	115.676	-0.890	-0.463	30.5	62.54
t (Dy়াস)	86.9407	110.848	12287.359	1.071	1.520	3	365
CS (MPa)	40.75	18.52	342.98	0.0174	0.77	7.98	92.93

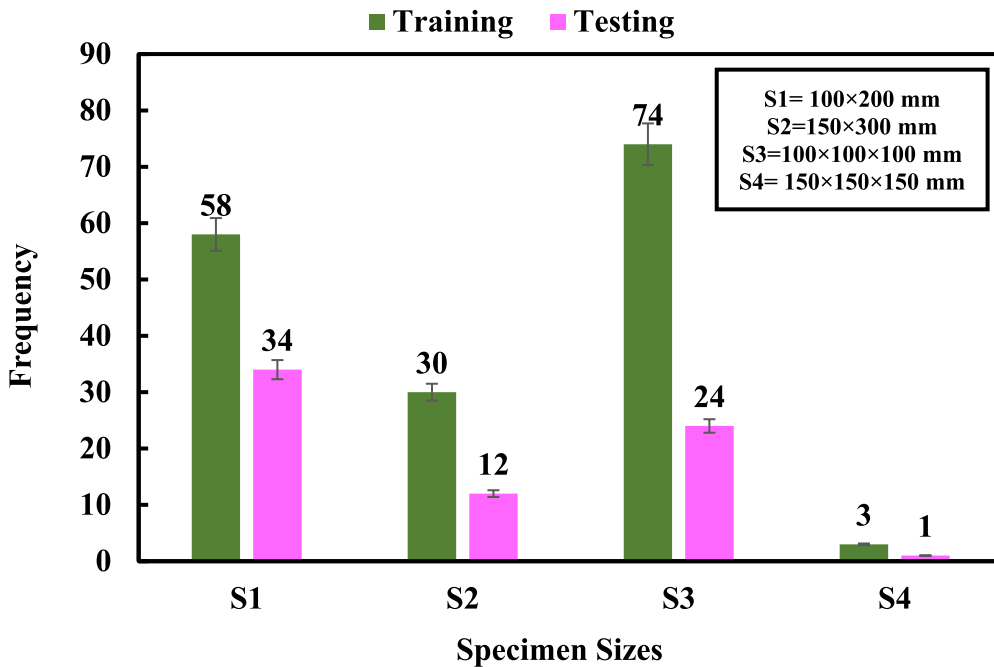


Fig. 5. A summary of the sample sizes utilized in training and testing for developing models.

### 3.5. Modeling

The correlation between dependent and independent variables establishes a direct relationship between the concrete mixture proportion and compressive strength. The datasets were randomly divided into training and testing datasets [38,39]. The training dataset is used to develop the models, whereas the testing dataset checks those developed models against unobserved data during training. Based on the correlation matrix, a poor correlation between independent variables such as CA, S, C, FA, CR, w/b, CaO, and SiO<sub>2</sub> and the dependent variable which is CS is observed as shown in Fig. 6. The correlations are 0.47, -0.30, 0.40, -0.23, -0.53, -0.58, -0.08, and -0.34, respectively. However, an acceptable correlation coefficient between CS and t is noticed by 0.75. Therefore, different multivariable models are advanced in the following section to establish an analytical model to predict the compressive strength of concrete.

#### 3.5.1. Full quadratic (FQ) model

Equation (2) shows the full quadratic formula, representing a relationship between compressive strength, the first and second degrees of each independent variable, and the interaction between independent variables [32,40–44]. This model is found to have a complex combination of mathematical terms [45,46].

$$\begin{aligned}
 CS = & \beta_1 + \beta_2(CA) + \beta_3(S) + \beta_4(C) + \beta_5(FA) + \beta_6(CR) + \beta_7\left(\frac{w}{b}\right) \\
 & + \beta_8(CaO) + \beta_9(SiO_2) + \beta_{10}(t) + \beta_{11}(CA)(S) + \beta_{12}(CA)(C) \\
 & + \beta_{13}(CA)(FA) + \beta_{14}(CA)(CR) + \beta_{15}(CA)\left(\frac{w}{b}\right) + \beta_{16}(CA)(CaO) \\
 & + \beta_{17}(CA)(SiO_2) + \beta_{18}(CA)(t) + \beta_{19}(S)(C) + \beta_{20}(S)(FA) \\
 & + \beta_{21}(S)(CR) + \beta_{22}(S)\left(\frac{w}{b}\right) + \beta_{23}(S)(CaO) + \beta_{24}(S)(SiO_2) + \beta_{25}(S)(t) \\
 & + \beta_{26}(C)(FA) + \beta_{27}(C)(CR) + \beta_{28}(C)\left(\frac{w}{b}\right) + \beta_{29}(C)(CaO) \\
 & + \beta_{30}(C)(SiO_2) + \beta_{31}(C)(t) + \beta_{32}(FA)(CR) + \beta_{33}(FA)\left(\frac{w}{b}\right) \\
 & + \beta_{34}(FA)(CaO) + \beta_{35}(FA)(SiO_2) + \beta_{36}(FA)(t) + \beta_{37}(CR)\left(\frac{w}{b}\right) \\
 & + \beta_{38}(CR)(CaO) + \beta_{39}(CR)(SiO_2) + \beta_{40}(CR)(t) + \beta_{41}\left(\frac{w}{b}\right)(CaO) \\
 & + \beta_{42}\left(\frac{w}{b}\right)(SiO_2) + \beta_{43}\left(\frac{w}{b}\right)(t) + \beta_{44}(CaO)(SiO_2) + \beta_{45}(CaO)(t) \\
 & + \beta_{46}(SiO_2)(t) + \beta_{47}(CA)^2 + \beta_{48}(S)^2 + \beta_{49}(C)^2 + \beta_{50}(FA)^2 + \beta_{51}(CR)^2 \\
 & + \beta_{52}\left(\frac{w}{b}\right)^2 + \beta_{53}(CaO)^2 + \beta_{54}(SiO_2)^2 + \beta_{55}(t)^2
 \end{aligned} \tag{2}$$

CS, CA, S, C, FA, CR, w/b, CaO, SiO<sub>2</sub>, and t are compressive strength, coarse aggregate content, fine aggregate content, cement content, fly ash content, cement replacement, water-to-binder ratio, calcium oxide

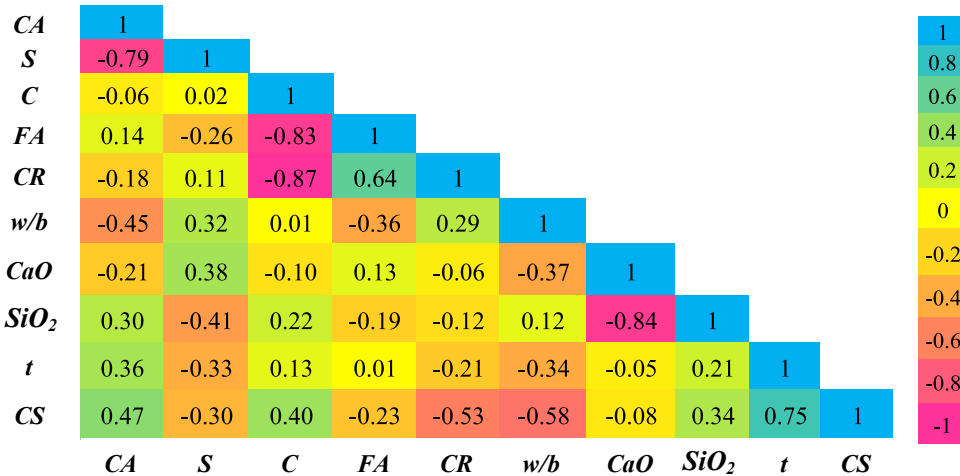


Fig. 6. Correlation matrix plot between the dependent and independent variables of concrete modified with fly ash.

ratio, silicon dioxide ratio, and curing time, respectively. Furthermore, the  $\beta_1$  to  $\beta_{55}$  are model parameters.

### 3.5.2. Nonlinear regression (NLR) model

The following formula is a typical form to develop a nonlinear regression model [32,47,48] for predicting the compressive strength of concrete containing different types of fly ash with various quantities of CaO and SiO<sub>2</sub>, Eq. (3). NLR model has a disadvantage which is the complex mathematical operation [49].

$$CS = \alpha_1(CA)^{\alpha_2} + \alpha_3(S)^{\alpha_4} + \alpha_5(C)^{\alpha_6} + \alpha_7(FA)^{\alpha_8} + \alpha_9(CR)^{\alpha_{10}} + \alpha_{11}\left(\frac{w}{b}\right)^{\alpha_{12}} + \alpha_{13}(CaO)^{\alpha_{14}} + \alpha_{15}(SiO_2)^{\alpha_{16}} + \alpha_{17}(t)^{\alpha_{18}} \quad (3)$$

CS, CA, S, C, FA, CR, w/b, CaO, SiO<sub>2</sub>, and t are compressive strength, coarse aggregate content, fine aggregate content, cement content, fly ash content, cement replacement, water-to-binder ratio, calcium oxide ratio, silicon dioxide ratio, and curing time, respectively. The  $\alpha_1$  to  $\alpha_{18}$  is defined as the model parameters.

### 3.5.3. Multi-linear regression (MLR) model

The compressive strength of the concrete containing different CaO and SiO<sub>2</sub> ratios is predicted using the multi-linear regression model. Equation (4) represents the product of the variables affecting the compressive strength of the concrete in exponential and constant terms. The MLR model has some advantages, such as simple mathematical operation and easy implementation resulting in more accurate results compared to the LR model. However, the MLR model greatly depends on the number of data; fewer number provides less accuracy. Therefore, this model has poor quality [32].

$$CS = \alpha_1(CA)^{\alpha_2}(S)^{\alpha_3}(C)^{\alpha_4}(FA)^{\alpha_5}(CR)^{\alpha_6}\left(\frac{w}{b}\right)^{\alpha_7}(CaO)^{\alpha_8}(SiO_2)^{\alpha_9}(t)^{\alpha_{10}} \quad (4)$$

Where  $\alpha_1$  to  $\alpha_{10}$  are defined as the model parameters

$$\begin{aligned} \beta_n = & a_n(CA) + b_n(S) + c_n(C) + d_n(FA) + e_n(CR) + f_n\left(\frac{w}{b}\right) + g_n(CaO) \\ & + h_n(SiO_2) + i_n(t) + b \end{aligned} \quad (5a)$$

$$CS = \frac{Node1}{1 + e^{-\beta_1}} + \frac{Node2}{1 + e^{-\beta_2}} + \dots + \frac{Node_n}{1 + e^{-\beta_n}} + Threshold \quad (5b)$$

### 3.5.4. Artificial neural network (ANN model)

The Artificial Neural Network (ANN) is a computational system that analyzes data like the human brain. This model is also a machine learning system used in construction engineering for various numerical forecasts and challenges [27,29,31,42]. ANN is made up of three layers; input, hidden, and output, which are linked by biases and weights [44,50], Eq. (5). This study designed a multi-layer feed-forward network with concrete components (CA, S, C, FA, CR, w/b, CaO, SiO<sub>2</sub>, and t) as input and CS as output. In the output layer, a sigmoid activation function is utilized.

$$Output = f\left(\sum_{j=1}^n w_j x_j + bias\right) \quad (5)$$

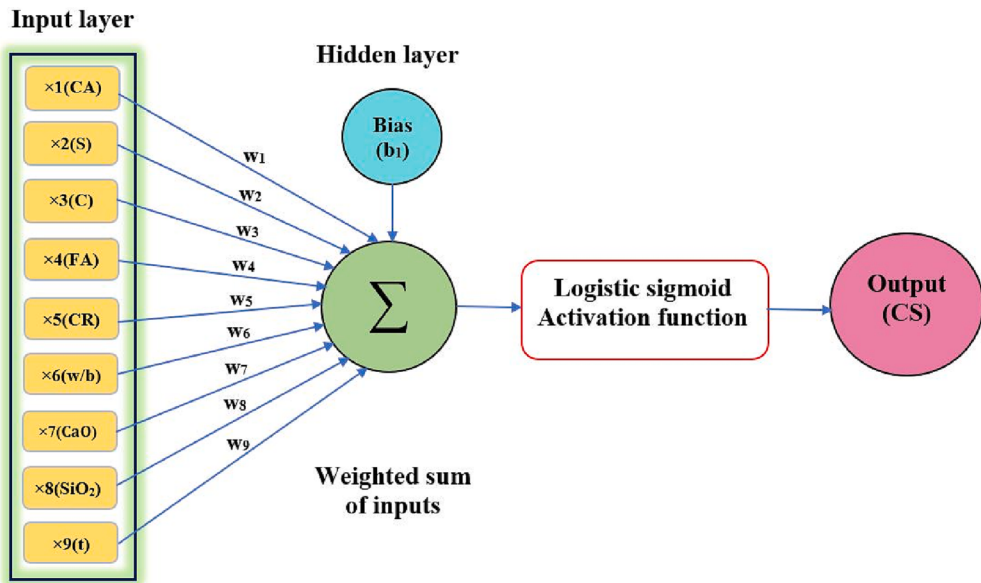
j is the number of input variables, x<sub>j</sub> is the input parameter, and bias is the threshold for the sigmoid activation function.

Fig. 7 shows the typical process of the ANN result. As well as the typical procedure for ANN calculation in a single hidden layer is illustrated in Eq. (5).

The Node1 to Node<sub>n</sub>, and Threshold are directly calculated.

### 3.6. Metrics to evaluate developed models

The developed models are evaluated using different parameters such as correlation coefficient ( $R^2$ ), root mean squared error (RMSE), mean absolute error (MAE), scatter index (SI), objectives (OBJ), and a20-index. The values of the a20-index are predicted to be unity for a perfect predictive model. The proposed a20-index has the advantage of having physical engineering meaning; it declares the number of samples that satisfy expected values with a 20% variance from experimental values [51]. The following equations (6)–(11) are utilized to determine each mentioned criterion [46,52–54].



**Fig. 7.** Typical ANN output technique in a single node.

$$R^2 = \left( \frac{\sum_i (yp - \bar{x}) \times (yi - \bar{y})}{\sqrt{\sum_i (yp - \bar{x})^2} \times \sqrt{\sum_i (yi - \bar{y})^2}} \right)^2 \quad (6)$$

$$RMSE = \sqrt{\frac{\sum_{i=1}^n (yi - yp)^2}{N}} \quad (7)$$

$$MAE = \frac{\sum_{i=1}^n |yi - yp|}{n} \quad (8)$$

$$SI = \frac{RMSE}{yi} \quad (9)$$

$$OBJ = \left( \frac{n_{tr}}{n_{all}} \times \frac{RMSE_{tr} + MAE_{tr}}{R_{tr}^2 + 1} \right) + \left( \frac{n_{tst}}{n_{all}} \times \frac{RMSE_{tst} + MAE_{tst}}{R_{tst}^2 + 1} \right) \quad (10)$$

$$a20 - index = \frac{N20}{N} \quad (11)$$

where;

$yp$  = predicted value of compressive strength.

$yi$  = experimental value of compressive strength.

$\bar{x}$  = mean of predicted compressive strength values.

$\bar{y}$  = mean of experimental compressive strength data.

$n_{tr}$  = number of the training dataset.

$n_{tst}$  = number of the testing dataset.

$n_{all}$  = a total number of datasets, including training and testing.

$N$  = total number of data in the dataset.

$N20$  = total number of predicted to the experimental data of compressive strength ratio ranged from 0.8 to 1.2.

The value of  $R^2$  and  $a-20$  index is commonly between (0to1), and the best value is considered 1. The RMSE, MAE, and OBJ values are between (0to∞), the value is recommended to be low as possible, and zero is the best value. As well as, if the value of SI was smaller than 0.1, the model is qualified as an excellent performance. Whereas the SI value is between (0.1 to 0.2), (0.2 to 0.3), and greater than 0.3, indicating the good, fair, and poor performance of the model, respectively [44,55].

#### 4. Results and discussion

##### 4.1. Variation of predicted and measured compressive strength

###### 4.1.1. FQ model

The full quadratic model is one of the most effective models due to its advanced mathematical expression. This model was used to predict the compressive strength of concrete modified with various fly ash types. It was derived based on mathematical parameters such as constant, linear, variable product terms/interaction, and squared variables. Equation (12) shows the formula for the FQ model for predicting the compressive strength of concrete. The correlation between predicted and measured compressive strength for the FQ model is illustrated in Fig. 8. The value of  $R^2$  and RMSE was 0.94 and 4.627 for training and 0.887 and 4.57 for testing data, respectively. The training dataset contains an error line of 15 to −15%, meaning that 85% of the data falls between 0.85 and 1.15 for the predicted to measured compressive strength ratio.

$$\begin{aligned} CS = & -1.26 - 0.17(CA) - 0.03(S) + 0.9(C) - 0.35(FA) - 1.36(CR) \\ & + 1.2\left(\frac{w}{b}\right) - 2.8(CaO) + 5.46(SiO_2) + 0.4(t) + 0.0002(CA)(S) \\ & - 0.0002(CA)(C) - 0.0002(CA)(FA) + 0.001(CA)(CR) \\ & - 0.05(CA)\left(\frac{w}{b}\right) + 0.0001(CA)(CaO) - 0.003(CA)(SiO_2) \\ & - 0.0003(CA)(t) - 0.0004(S)(C) - 0.001(S)(FA) + 0.00003(S)(CR) \\ & - 0.19(S)\left(\frac{w}{b}\right) + 0.003(S)(CaO) + 0.0012(S)(SiO_2) - 0.0004(S)(t) \\ & + 0.002(C)(FA) - 0.0003(C)(CR) - 0.18(C)\left(\frac{w}{b}\right) - 0.0007(C)(CaO) \\ & - 0.0097(C)(SiO_2) - 0.0002(C)(t) + 0.004(FA)(CR) + 0.48(FA)\left(\frac{w}{b}\right) \\ & - 0.004(FA)(CaO) - 0.005(FA)(SiO_2) - 0.001(FA)(t) \\ & - 0.16(CR)\left(\frac{w}{b}\right) + 0.04(CR)(CaO) + 0.002(CR)(SiO_2) \\ & + 0.003(CR)(t) + 1.95\left(\frac{w}{b}\right)(CaO) + 0.04\left(\frac{w}{b}\right)(SiO_2) - 0.26\left(\frac{w}{b}\right)(t) \\ & - 0.03(CaO)(SiO_2) + 0.001(CaO)(t) + 0.6(SiO_2)(t) \\ & + 0.0001(CA)^2 - 0.000002(S)^2 - 0.0005(C)^2 + 0.001(FA)^2 \\ & - 0.0003(CR)^2 + 0.0001\left(\frac{w}{b}\right)^2 + 0.0001(CaO)^2 \\ & + 0.0004(SiO_2)^2 - 0.0003(t)^2 \end{aligned} \quad (12)$$

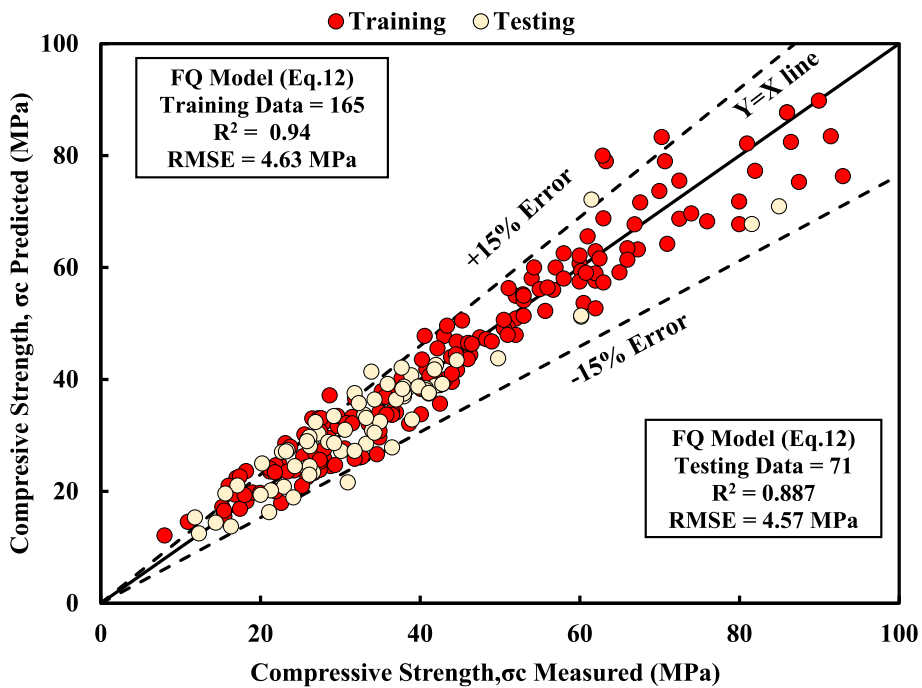


**Fig. 8.** Comparison between measured and predicted CS using FQ model for training and testing dataset.

No. of training dataset = 165,  $R^2 = 0.94$ , RMSE = 4.627 MPa.

#### 4.1.2. NLR model

The nonlinear regression model was also used to predict the compressive strength of fly ash-modified concrete. The NLR model result is shown in Eq. (13). The relationship between predicted and measured compressive strength is displayed in Fig. 9. The training dataset has an  $R^2$  and RMSE value of 0.816 and 8.36 MPa. Also, an  $R^2$  of 0.47 and RMSE of 9.62 MPa for the testing dataset were observed. According to the RMSE results, the NLR model performance is fair. The FQ model results

counted as one of the least effective models due to its elementary mathematical expression. The MLR model formula consists of constant terms with terms that rose to the power of constant variables. The following equation presents the variables and their relationship in detail; Eq. (14). The relation between predicted and measured compressive strength is illustrated in Fig. 10. The  $R^2$  and RMSE were 0.79 and 9.22 for training, 0.61 and 8.25 for testing data, respectively. The error line in the training dataset is 25 to -25%, which means that 75% of the data falls between 0.75 and 1.25 for the projected to measured compressive strength ratio.

$$CS = 1.3 (CA)^{0.8} (S)^{0.35} (C)^{0.16} (FA)^{0.18} (CR)^{-0.74} \left(\frac{W}{b}\right)^{-0.05} (CaO)^{0.37} (SiO_2)^{0.2} + (t)^{0.0000002} \quad (14)$$

provide better performance than the NLR model. The error line in the training dataset is 30 to -30%, which means that 70% of the data falls between 0.7 and 1.3 for the predicted to measured compressive strength ratio.

No. of training dataset = 165,  $R^2 = 0.79$ , RMSE = 9.22 MPa.

$$CS = 140.66 (CA)^{-0.008} + 0.68(S)^{-2.47} + 1.06(C)^{0.0002} - 0.041(FA)^{0.002} - 3.096(CR)^{-6.87} + 13.94 \left(\frac{W}{b}\right)^{-1.14} - 26.95 (CaO)^{-0.004} - 227(SiO_2)^{-0.146} + 5.32 (t)^{0.35} \quad (13)$$

No. of training dataset = 165,  $R^2 = 0.816$ , RMSE = 8.36 MPa.

#### 4.1.3. MLR model

The multi-linear regression model is another model utilized to predict the compressive strength of concrete modified with fly ash. It is

#### 4.1.4. ANN model

The Optimum ANN network structure is the last model used to predict the compressive strength of concrete. Five trials were selected depending on the RMSE and MAE values, as shown in Fig. 11. Among those five trials, the lowest RMSE and MAE values were observed in the

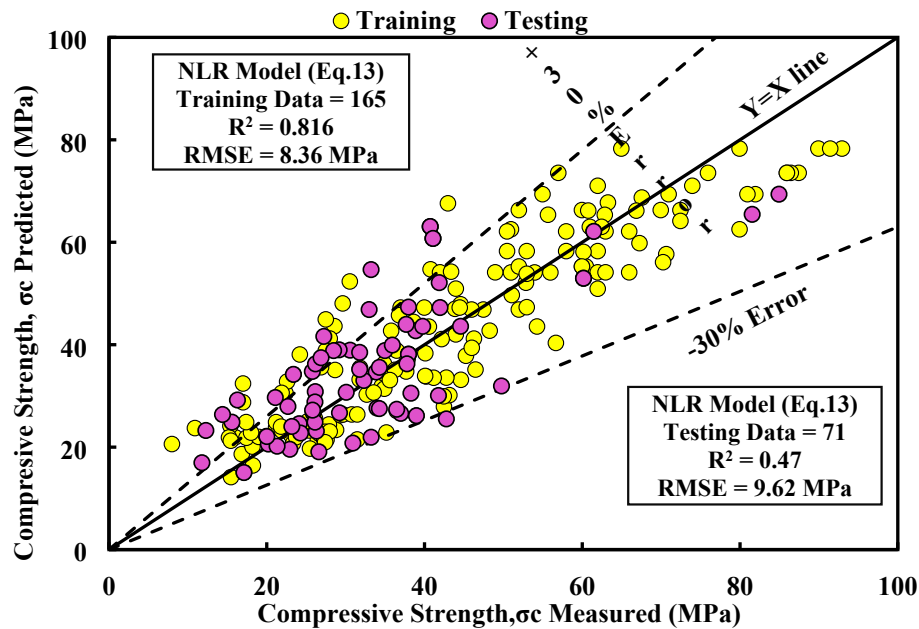


Fig. 9. Comparison between measured and predicted CS using NLR model for training and testing dataset.

network containing one hidden layer with 19 neurons. The ANN network having one hidden layer with 19 neurons with 0.1 of momentum, a learning rate of 0.2, and 2000 learning time, is chosen, Fig. 12. The ANN formula, including weights and biases, is shown in Eq. (15). Fig. 13 shows the relation between predicted compressive strength by the ANN having 19 neurons with the experimental compressive strength values for both training and testing data. ANN network analysis has an  $R^2$  of 0.987 and RMSE of 3.3 MPa when the training data are applied. The model provides an  $R^2$  of 0.986 and RMSE of 3.52 MPa when testing data is used. The training dataset has an error line of 10 to  $-10\%$ , indicating that 90% of the data are laid between 0.9 and 1.1 for the ratio of predicted compressive strength to measured compressive strength. As well as Fig. 13 shows the variation between measured and predicted compressive strength values plotted for different strength ranges based on the training dataset. The highest value of  $R^2$  was found in the CS of 65 to 95 MPa.

$$CS = -\frac{0.1}{1 + e^{-\beta_1}} - \frac{0.02}{1 + e^{-\beta_2}} - \frac{0.15}{1 + e^{-\beta_3}} - \dots - \frac{0.95}{1 + e^{-\beta_{19}}} + 0.475 \quad (15)$$

No. of training dataset = 165,  $R^2 = 0.987$ , RMSE = 3.3 MPa.

#### 4.2. Effect of $CaO$ and $SiO_2$ content on the compressive strength of concrete

The FQ model was used to examine the influence of cement replacement percentage,  $CaO$  (%), and  $SiO_2$  (%) on cement-based concrete's compressive strength using a fly-ash modified concrete dataset. All independent parameters were held constant, and the CR was increased from 18 to 100%; the compressive strength grew as the cement replacement increased. The  $SiO_2$  (%) was then increased from 30.5 to 62.54% while the CA, S, C, FA, w/b,  $CaO$ , and t remained constant. According to the model results, increasing  $SiO_2$  causes a gradual increase in compressive strength, while  $CaO$  (%) ranges between 0.3 and

-0.699	-0.034	0.187	0.099	0.278	0.126	0.156	-0.032	0.423	-1.770	$\beta_1$
-0.674	-0.024	0.141	0.107	0.324	-0.007	0.186	0.074	0.431	-1.815	$\beta_2$
-0.719	-0.082	0.065	0.552	0.144	0.343	0.227	-0.089	0.294	-1.644	$\beta_3$
-0.9	0.062	0.136	-0.093	0.332	0.132	-0.098	-0.26	0.482	-1.673	$\beta_4$
-2.249	-0.093	0.085	0.059	-0.422	-0.77	-1.588	1.53	0.384	-2.852	$\beta_5$
-0.787	0.044	0.099	0.052	0.353	0.371	-0.033	-0.262	0.355	-1.656	CA
-0.618	0.074	-0.137	0.399	0.459	0.824	-0.182	-0.597	0.042	-1.569	S
-0.73	-0.084	0.111	0.382	0.201	0.36	0.248	-0.048	0.415	-1.618	C
1.067	2.077	0.468	-1.587	-0.042	-2.883	-0.566	-0.952	0.889	-3.131	FA
-0.406	-0.46	-0.089	0.705	-0.152	-0.003	1.294	-0.354	-2.561	-1.826	$\times$
-0.152	-0.16	1.543	0.415	-1.948	1.465	-1.387	0.046	-1.439	-2.373	w/b
-1.143	0.245	0.73	-0.905	0.052	-0.04	-0.104	0.063	1.198	-1.805	$\beta_{11}$
-0.738	-0.034	0.023	0.399	0.242	0.285	0.069	-0.22	0.281	-1.661	$CaO$
-0.668	-0.034	0.176	0.143	0.353	-0.051	0.166	0.082	0.432	-1.823	$\beta_{12}$
-0.78	-0.06	0.129	0.086	0.294	0.113	0.087	-0.125	0.394	-1.743	t
0.151	0.712	-1.587	2.137	0.13	1.045	-1.958	1.349	0.004	-3.212	$\beta_{13}$
-0.698	-0.092	0.07	0.326	0.213	0.276	0.283	0.036	0.479	-1.556	$\beta_{14}$
-0.714	-0.083	0.061	0.538	0.143	0.278	0.338	0.059	0.446	-1.637	$\beta_{15}$
-0.734	-0.071	0.145	0.186	0.0274	0.293	0.151	-0.129	0.373	-1.678	$\beta_{16}$
										$\beta_{17}$
										$\beta_{18}$
										$\beta_{19}$

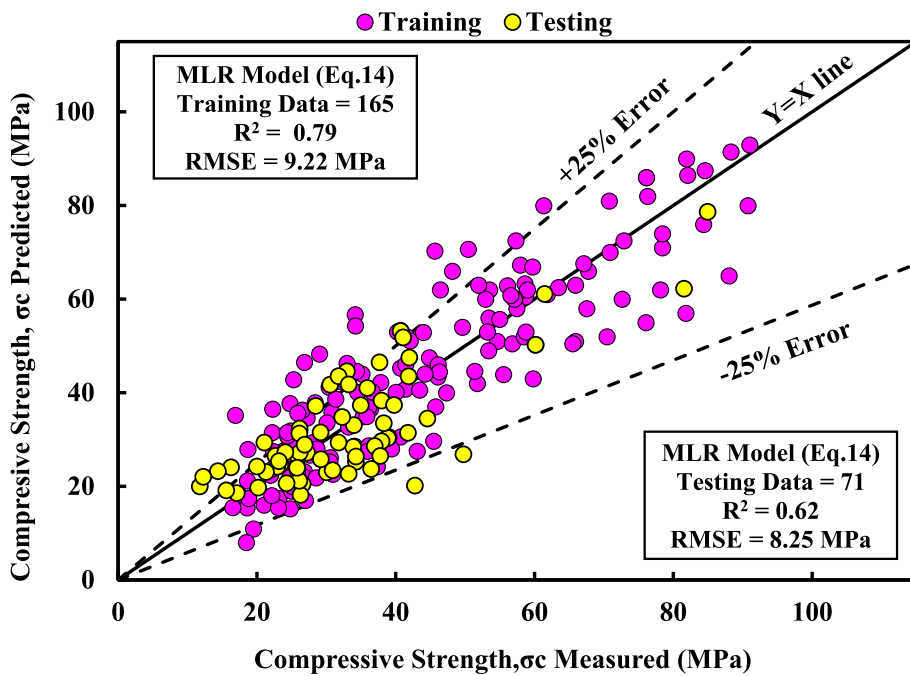


Fig. 10. Comparison between measured and predicted CS using MLR model for training and testing dataset.

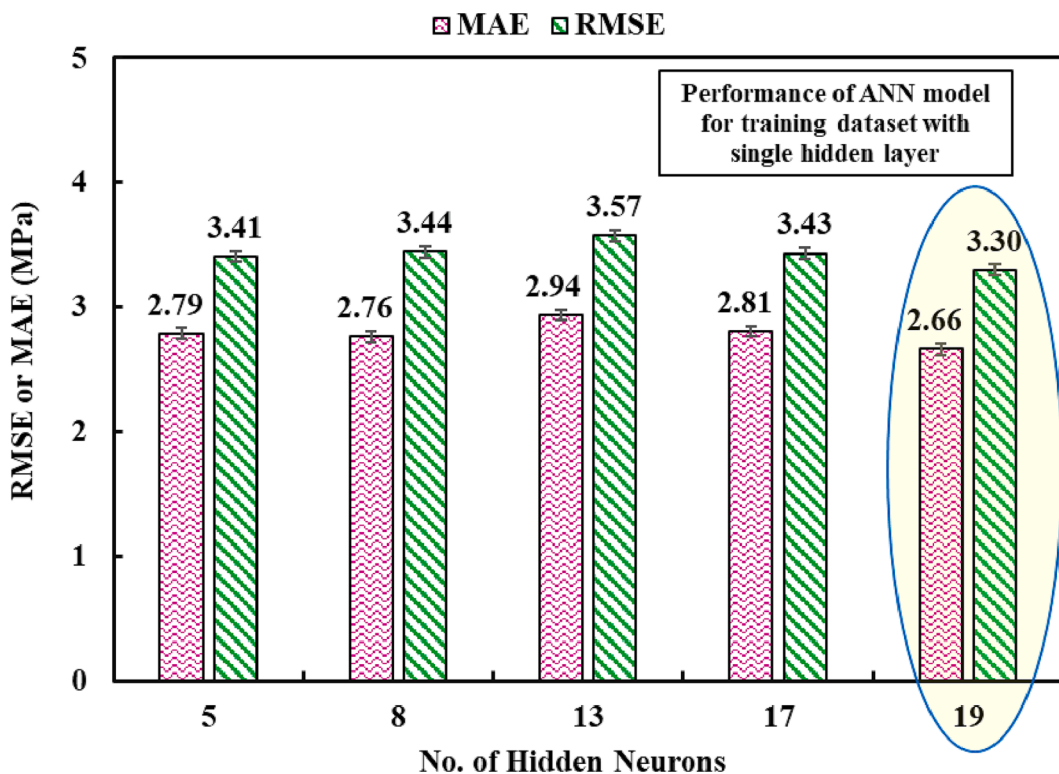


Fig. 11. Selecting optimum ANN based on RMSE and MAE.

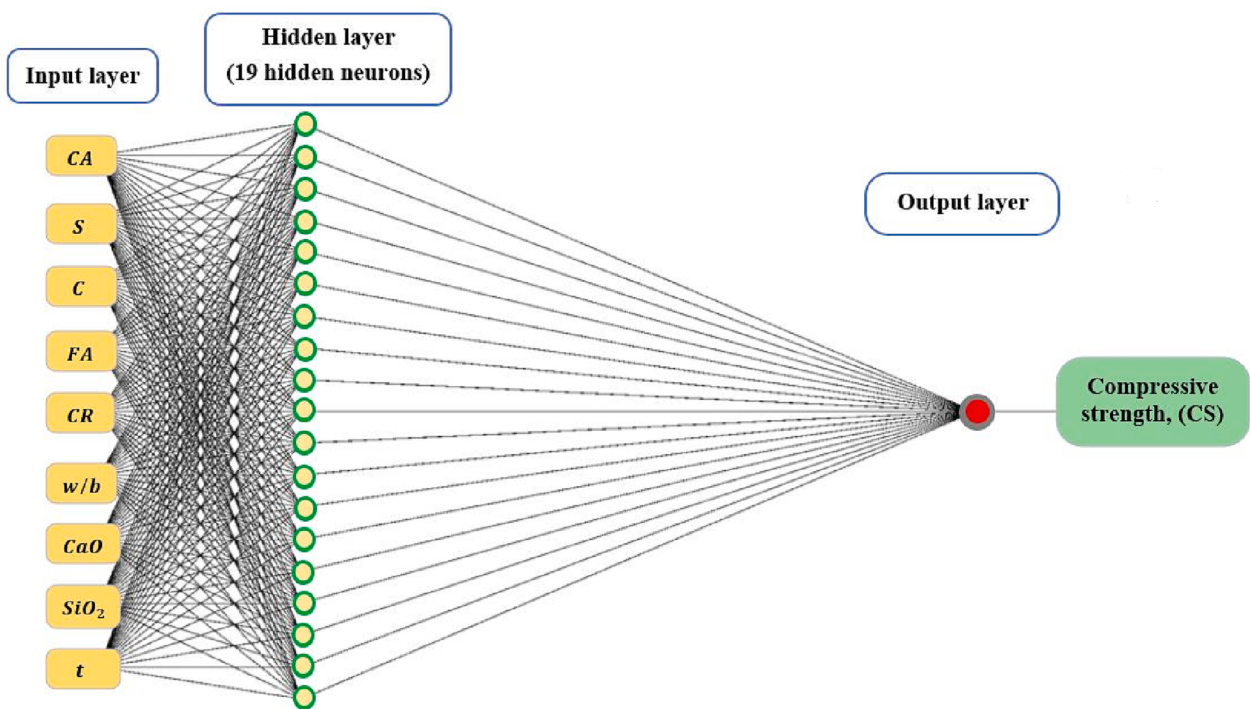


Fig. 12. Optimal ANN network structures containing one hidden layer and 19 hidden neurons.

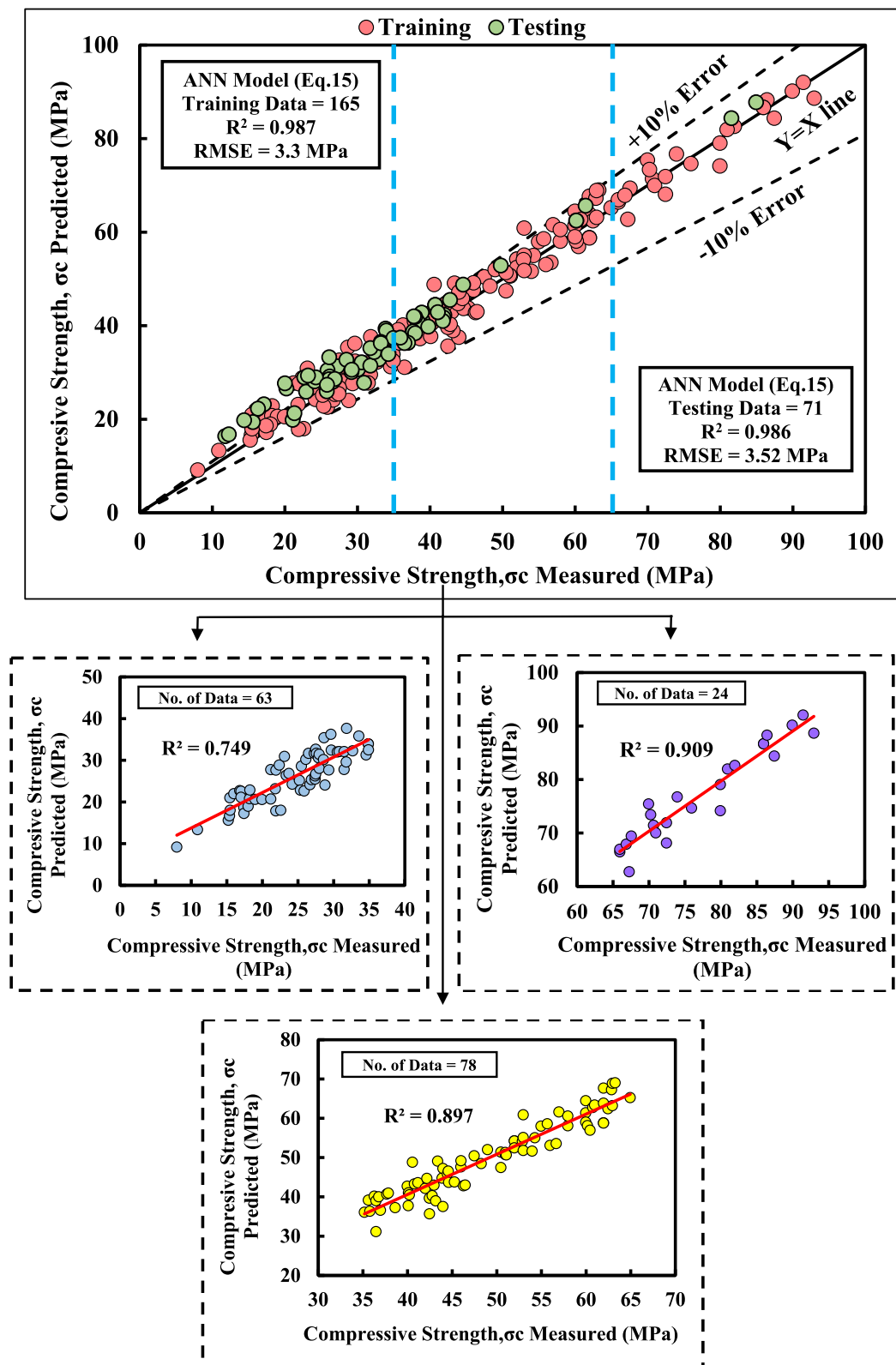
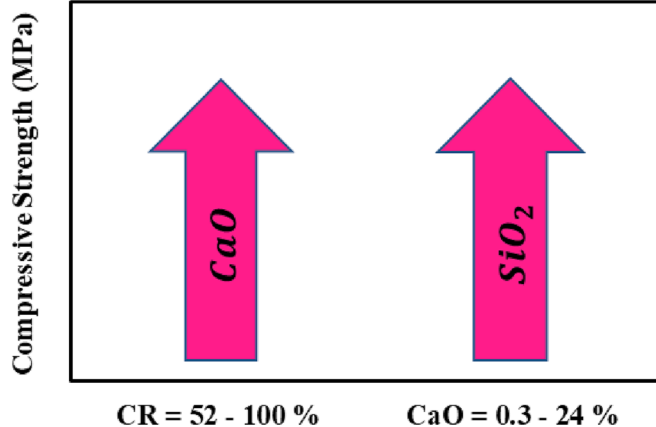


Fig. 13. Comparison between measured and predicted CS using ANN model for training and testing dataset.



**Fig. 14.** The effect of CaO and SiO<sub>2</sub> content of fly ash on the compressive strength of concrete.

24% but contributes a reduction above that. To determine the influence of CaO (%), all other parameters were fixed, including CA, S, C, FA, CR, w/b, and SiO<sub>2</sub>, and the CaO (%) varied from 0.3 to 31.9%. Concrete compressive strength improved as the CaO (%) increased, but only when the cement replacement was between 52 and 100% and dropped below that. **Fig. 14** depicts the performance of CaO and SiO<sub>2</sub>.

##### 5. Evaluation of developed models

The study attempted to determine the effect of two major chemical compositions of fly ash, CaO, and SiO<sub>2</sub>, on the compressive strength of cement-based concrete modified with various types and amounts of fly ash. The experiment includes forecasting concrete compressive strength using four alternative models; FQ, NLR, MLR, and ANN. Each model supplied a formula based on several mathematical parameters. To evaluate the performance of each constructed model, various assessment criteria were applied.

According to the R<sup>2</sup>, RMSE, and MAE statistics, the ANN model has the maximum accuracy and reliability for prediction using the training and testing dataset. **Table 3** summarizes the statistical criteria outcomes for the created models. The ANN model has an R<sup>2</sup> of 0.987, RMSE of 3.3 MPa, and MAE of 2.662 MPa based on the training dataset, as well as R<sup>2</sup> of 0.986, RMSE of 3.52 MPa, and MAE of 2.96 MPa for the testing dataset.

Furthermore, more data are along the Y = X line for the ANN model, which has an error line of 10 to -10% for the training dataset, referring to the fact that 90% of the data are between 0.90 and 1.1 (predicted CS/measured CS). The second-ranked model is the FQ model; it has an R<sup>2</sup> of 0.94, RMSE of 4.627 MPa, and MAE of 3.496 MPa for the training dataset, and R<sup>2</sup> of 0.887, RMSE of 4.57 MPa, and MAE of 3.457 for the testing dataset. The FQ model has an error line of  $\pm$  15 for the training dataset. The NLR and MLR model have error lines of  $\pm$  30, and  $\pm$  25, respectively, indicating the model's poor performance. **Fig. 15** compares created models based on the testing dataset; model values are within the  $\pm$  20 and  $\pm$  30% error lines.

The training dataset for the models based on three different CS ranges was plotted, and the RMSE values were provided. **Table 4** shows

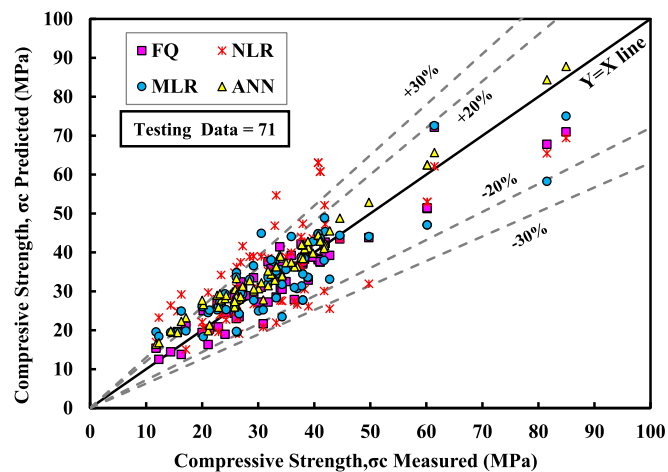


**Fig. 15.** Variation of measured and predicted CS for developed models using the testing dataset.

**Table 4**

Root mean squared error (RMSE) for the developed models in different ranges of compressive strength.

Compressive Strength range (MPa)	No. of data	Models			Best Model Performance
		FQ	NLR	MLR	
5 to 34	63	3.731	7.723	6.335	3.576 ANN
35 to 64	78	4.312	8.231	10.599	3.16 ANN
65 to 95	24	7.087	10.21	10.686	2.616 ANN

an overview of the findings. There were 63 datasets for the strength range of 5 to 34 MPa, 78 in the range of 65 to 95 MPa, and 24 data for the 65 to 95 MPa. According to the findings, the ANN model was more appropriate than other models for all CS ranges. The model provided an RMSE of 3.576, 3.16, and 2.616 MPa for 5 to 34, 35 to 65, and 65 to 95 MPa, respectively.

The same models were employed to identify the ideal specimen shape and size. The dataset for each size specimen was modeled based on training and testing datasets. **Table 5** shows RMSE values for different models. According to the table, based on a satisfied number of data, the cylinder specimens with dimensions of 100\*200 mm have the lowest RMSE value, 0.124 MPa, for the training dataset using the ANN model. Although, the cylinder specimens with 150\*300 mm dimensions have the lowest value of RMSE for the testing dataset, which is 0.01 MPa.

Furthermore, the created models using the training and testing dataset were also evaluated by comparing the OBJ function and SI values. The highest value of SI is 0.104 for training, and the ANN model, **Fig. 16**, concluded 0.074 for testing. The model also has the lowest OBJ function compared to the other models, indicating that the model is more accurate in forecasting the compressive strength of concrete modified with fly ash. The model has an OBJ value of 3.09 and 1.0 MPa based on the training and testing dataset, respectively, **Fig. 17**. Although, the highest a-20 index value was observed for the MLR model; 104.4% for the training and 104.8% for the testing dataset, **Fig. 18**.

**Table 3**  
Summary of performance evaluation parameters for the developed models.

Models	Fig. (No)	Eq. (No.)	Training R <sup>2</sup>	RMSE (MPa)	MAE (MPa)	Testing R <sup>2</sup>	RMSE (MPa)	MAE (MPa)	Ranking
FQ	8	12	0.94	4.63	3.496	0.887	4.57	3.457	2
NLR	9	13	0.816	8.36	6.698	0.47	9.62	7.522	3
MLR	10	14	0.79	9.22	7.199	0.62	8.25	6.665	4
ANN	13	15	0.987	3.3	2.662	0.986	3.52	2.96	1

**Table 5**

Root mean squared error (RMSE) of the developed models using different specimen sizes and conducting.

Dataset	Sample size (mm)	No. of Samples	Models	NLR	MLR	ANN	Best Model Performance
			FQ				
Training	S1(100*200)	58	3.746	4.757	5.479	1.124	ANN
	S2(150*300)	30	2.363	6.592	6.008	2.512	ANN
	S3(100*100*100)	74	3.663	8.48	5.428	1.94	ANN
	S4(150*150*150)	3	NA	3.673	11.2	0	ANN
Testing	S1(100*200)	34	3.864	6.696	5.287	1.116	ANN
	S2(150*300)	12	10.179	6.592	5.196	0.01	ANN
	S3(100*100*100)	24	6.108	12.186	8.377	1.94	ANN
	S4(150*150*150)	1	N.A	6	3.54	0	ANN

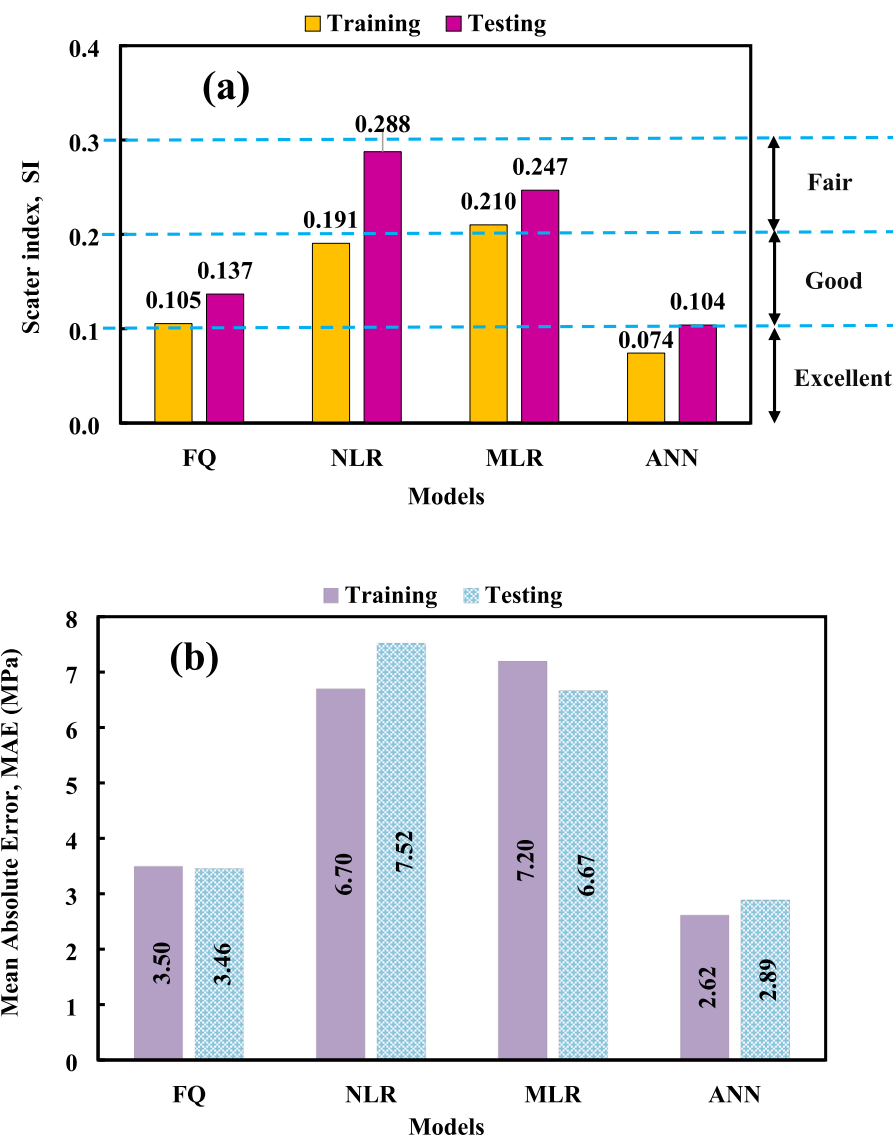


Fig. 16. Comparison of developed models using (a) SI and (b) MAE.

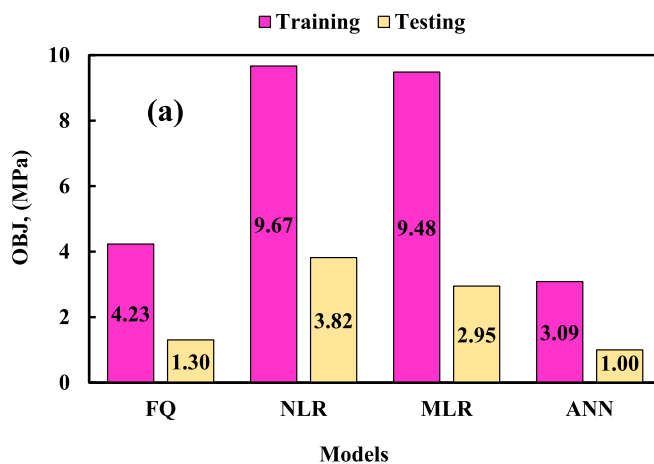


Fig. 17. Comparison of developed models using the OBJ function.

In addition, the created models were compared using residual error, as shown in Fig. 19. The residual error value is obtained by subtracting the expected compressive strength from the measured compressive strength. The results show that the FQ model has the lowest error value, ranging from  $-16.58$  to  $+17.14$  MPa. At the same time, the residual error for the NLR, MLR, and ANN models is  $-17.81$  to  $+24.64$  MPa,  $-24.61$  to  $+24.85$  MPa, and  $-6.80$  to  $+8.28$  MPa, respectively.

## 6. Sensitivity investigation

A sensitivity analysis was performed to evaluate the influence of each independent parameter on the value of modeled dependent variable [32,44,56,57]. To determine the sensitivity index of each parameter on the developed model, one parameter was extracted each time for the training data. The ANN was used for the sensitivity investigation as it was observed as the best model for predicting the compressive strength of concrete compared to the other conducted models. All  $R^2$ , RMSE, and MAE values were reported for each trial. The sensitivity results are shown in Table 6. The findings indicate that the curing time is the most

significant and influential parameter for predicting the compressive strength of concrete, Fig. 20.

## 7. Conclusions

To find an accurate and reliable model to predict the compressive strength of cement concrete modified with different fly ash types and quantities, 236 data samples for fly ash-modified cement concrete with different mixture proportions, CaO and SiO<sub>2</sub> quantity of fly ash, aggregate content, cement content, cement replacement, water-to-binder ratio, and curing time were collected from previous researches. According to the collected data and the result of four different model approaches, the following can be drawn:

The cement replacement percentage ranged between 18 and 100%. The compressive strength of concrete gradually increased when the replacement (%) was increased.

The data collected from various research studies show that CaO (%) varied between 0.3 and 31.9%. SiO<sub>2</sub> (%) ranged between 30.5 and 62.54%.

Increasing CaO (%) in fly ash caused an increase in compressive strength only when the cement replacement ranged between 52 and 100%. The CS also improved with increasing SiO<sub>2</sub> (%), where; the CaO (%) varied between 0.3 and 24%.

Based on multiple assessment criteria such as  $R^2$ , RMSE, and MAE, the ANN model showed the best accuracy and performance for predicting the compressive strength of concrete. The model had the highest value of  $R^2$ , which was 0.987 and 0.986 for training and testing datasets, respectively. The lowest value of RMSE and MAE was found as 3.3 and 2.66 for training, and 3.53 and 2.96 for testing, respectively.

Related to other statistical tools, such as SI and OBJ, the ANN model was first ranked. The SI and OBJ function values were 0.104 and 3.09 MPa for training and 0.074 and 1.0 MPa for the testing dataset, respectively. Although the highest a-20 index was observed for the MLR model, the value was 104.4% for the training dataset.

According to the shape and size of specimens, the cylinder specimens having 100\*200 mm were obtained for the best performance using the ANN model.

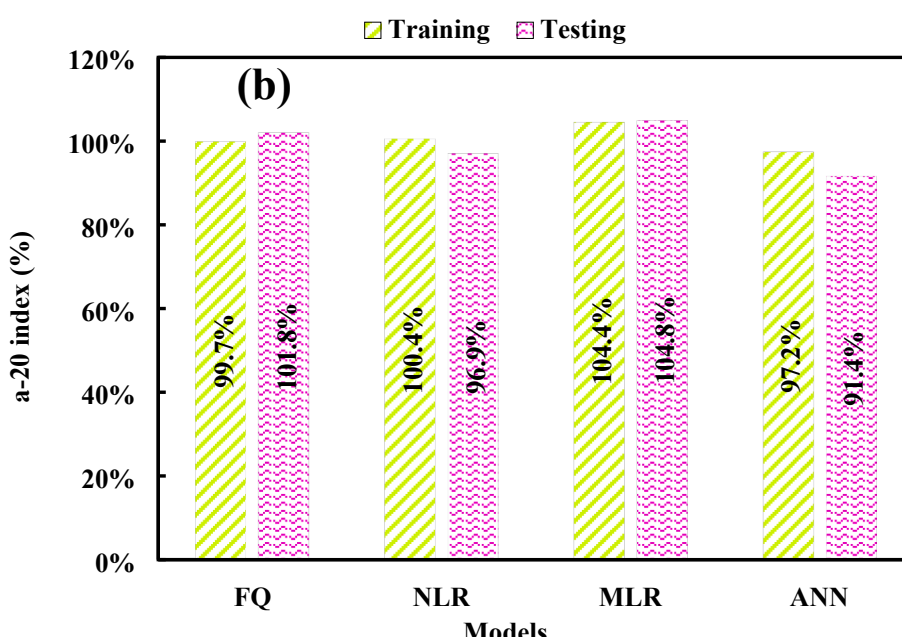
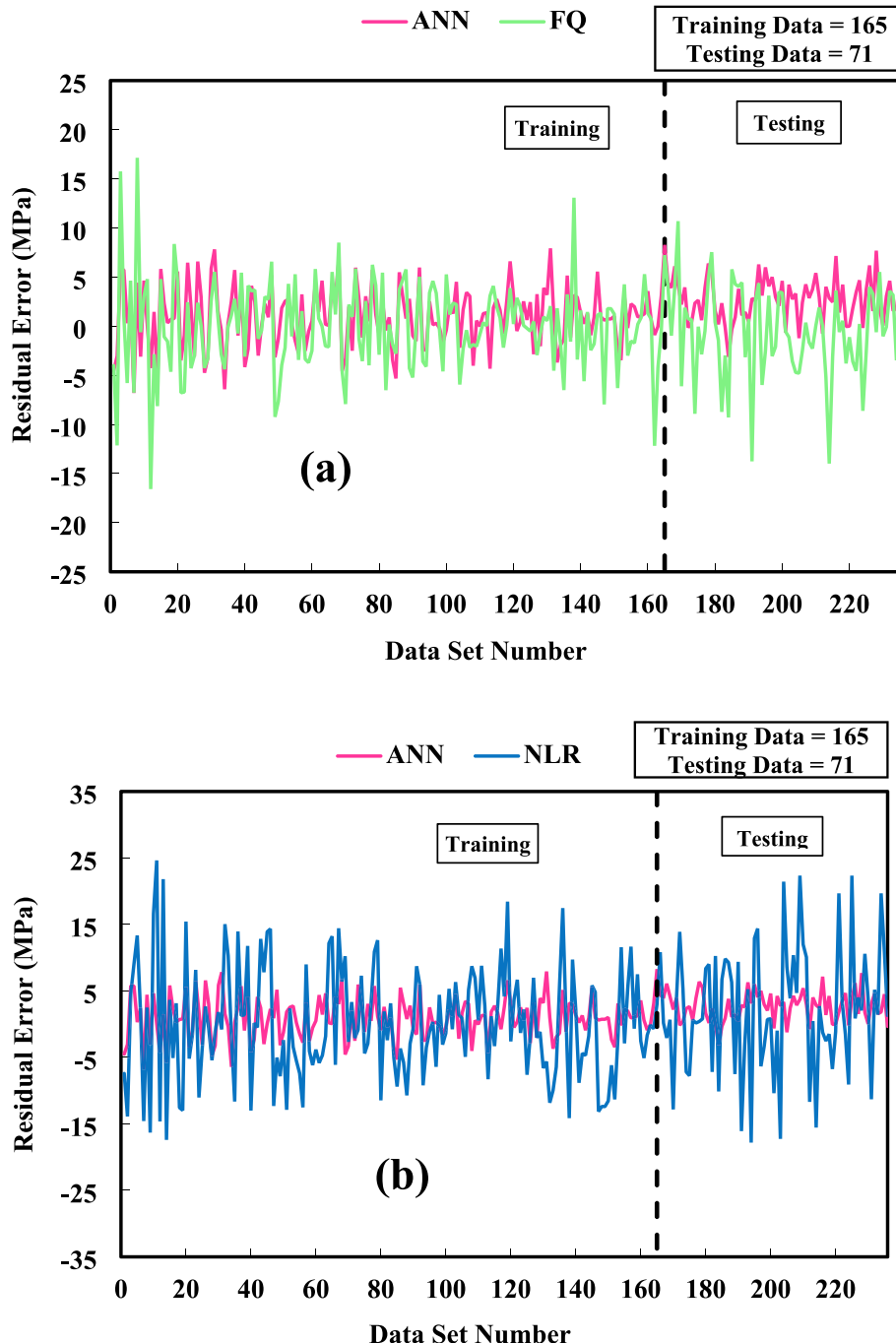


Fig. 18. Comparison of developed models using a20-index.



**Fig. 19.** Variation between measured and predicted CS for developed models based on residual error (a) ANN and FQ, (b) ANN and NLR, and (c) ANN and MLR.

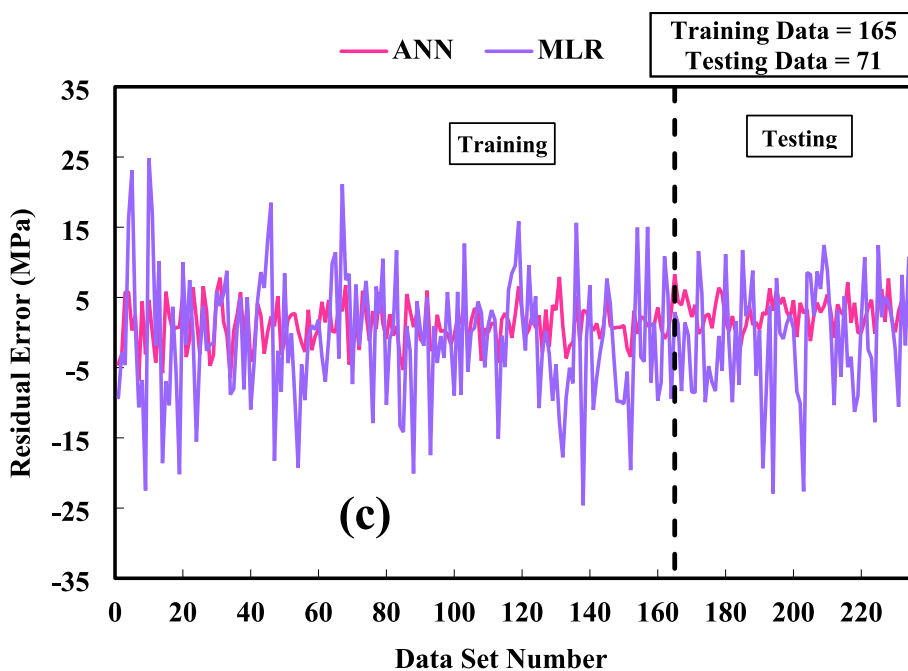


Fig. 19. (continued).

**Table 6**

Sensitivity analysis using the ANN model applied to the training dataset.

No.	Combination	Removed Parameter	R <sup>2</sup>	RMSE (MPa)	MAE (MPa)	Ranking based on RMSE and MAE
1	CA, S, C, FA, CR, w/b, CaO, SiO <sub>2</sub> , t	—	0.987	3.30	2.662	—
2	S, C, FA, CR, w/b, CaO, SiO <sub>2</sub> , t	CA	0.987	3.984	3.254	3
3	CA, C, FA, CR, w/b, CaO, SiO <sub>2</sub> , t	S	0.989	3.045	2.497	7
4	CA, S, FA, CR, w/b, CaO, SiO <sub>2</sub> , t	C	0.990	3.800	3.165	4
5	CA, S, C, CR, w/b, CaO, SiO <sub>2</sub> , t	FA	0.989	3.127	2.514	6
6	CA, S, C, FA, w/b, CaO, SiO <sub>2</sub> , t	CR	0.990	3.800	3.165	4
7	CA, S, C, FA, CR, CaO, SiO <sub>2</sub> , t	w/b	0.976	4.424	3.446	2
8	CA, S, C, FA, CR, w/b, SiO <sub>2</sub> , t	CaO	0.990	2.800	2.217	8
9	CA, S, C, FA, CR, w/b, CaO, t	SiO <sub>2</sub>	0.989	3.523	2.824	5
10	CA, S, C, FA, CR, w/b, CaO, SiO <sub>2</sub>	t	0.876	10.450	8.109	1

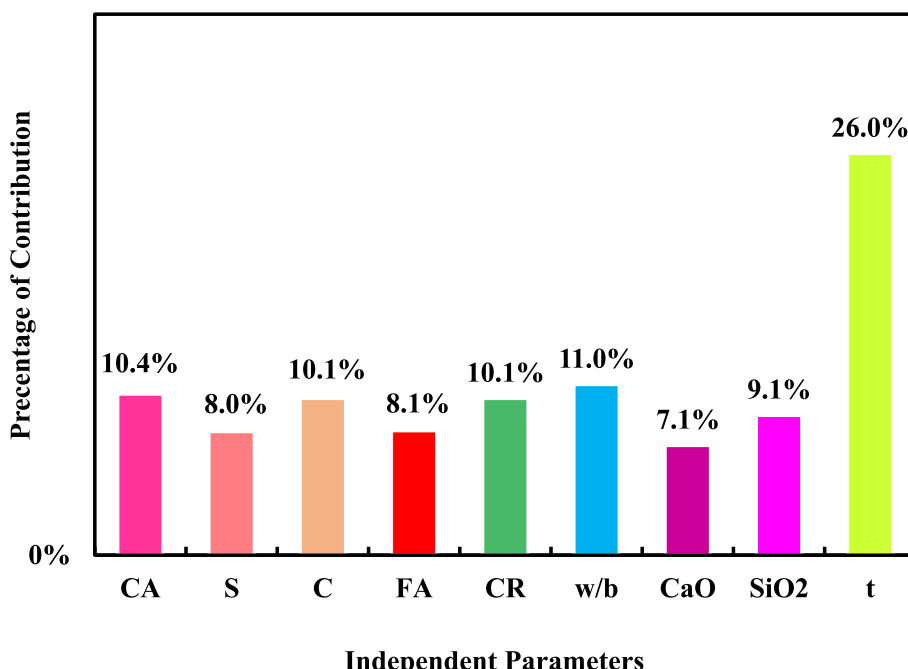


Fig. 20. The percentage contribution of input variables in predicting compressive strength of concrete using the ANN model.

The ANN model was applied to different CS ranges of concrete. The best performance of the model was observed in the range of 35 to 64 MPa.

Sensitivity analysis illustrates the most effective parameter for predicting the compressive strength of concrete: the curing time.

Using multiple models provides construction professionals with broader information and insights. This enhances decision-making processes by considering different perspectives and approaches, leading to more informed and effective decisions throughout the project lifecycle.

Employing multiple models allows for the validation and cross-verification of results. By comparing the predictions and outcomes of different models, construction practitioners can assess the accuracy and reliability of the models in different scenarios, increasing confidence in the results.

The construction industry is diverse, and no single model can address all situations. Applying multiple models acknowledges this diversity and provides the flexibility to choose the most appropriate model for specific projects, materials, or contexts. It enables the construction industry to adapt to evolving needs and challenges.

The use of multiple models encourages continuous improvement in construction practices. By comparing and evaluating different models, areas for improvement can be identified, leading to advancements in modeling techniques, data collection, and analysis methodologies. This fosters innovation and progress within the industry.

Discuss the advantages of machine learning models in the context of compressive strength prediction. These may include their ability to capture complex relationships, handle large datasets, adapt to different scenarios, and potentially provide better accuracy than traditional analytical models.

## Funding

This work had no finding.

## CRediT authorship contribution statement

**Dilshad Kakasor Ismael Jaf:** . **Payam Ismael Abdulrahman:** . **Ahmed Salih Mohammed:** . **Rawaz Kurda:** Investigation, Visualization. **Shaker M.A. Qaidi:** Validation. **Panagiotis G. Asteris:** Supervision, Writing – original draft, Writing – review & editing.

## Declaration of Competing Interest

The authors declare that they have no known competing financial interests or personal relationships that could have appeared to influence the work reported in this paper.

## Data availability

Data will be made available on request.

## References

- [1] B. Suhendro, Toward green concrete for better sustainable environment, Procedia Eng. 95 (2014) 305–320.
- [2] M.E. Bildirici, Cement production, environmental pollution, and economic growth: evidence from China and USA, Clean Techn. Environ. Policy 21 (4) (2019) 783–793.
- [3] S. Joel, Compressive strength of concrete using fly ash and rice husk ash: A review, Civ Eng J 6 (7) (2020) 1400–1410.
- [4] Ganesh Prabhu, G., Bang, J. W., Lee, B. J., Hyun, J. H., & Kim, Y. Y. (2015). Mechanical and durability properties of concrete made with used foundry sand as fine aggregate. *Advances in Materials Science and Engineering*, 2015.
- [5] T. Ayub, S.U. Khan, F.A. Memon, Mechanical characteristics of hardened concrete with different mineral admixtures: a review, Scientific World Journal 2014 (2014) 1–15.
- [6] I. Ignjatović, Z. Sas, J. Dragaš, J. Somlai, T. Kovács, Radiological and material characterization of high volume fly ash concrete, J. Environ. Radioact. 168 (2017) 38–45.
- [7] C. Herath, C. Gunasekara, D.W. Law, S. Setunge, Performance of high volume fly ash concrete incorporating additives: A systematic literature review, Constr. Build. Mater. 258 (2020), 120606.
- [8] R. Siddique, Utilization of silica fume in concrete: Review of hardened properties, Resour. Conserv. Recycl. 55 (11) (2011) 923–932.
- [9] S.C. Pal, A. Mukherjee, S.R. Pathak, Investigation of hydraulic activity of ground granulated blast furnace slag in concrete, Cem. Concr. Res. 33 (9) (2003) 1481–1486.
- [10] R. Khan, A. Jabbar, I. Ahmad, W. Khan, A.N. Khan, J. Mirza, Reduction in environmental problems using rice-husk ash in concrete, Constr. Build. Mater. 30 (2012) 360–365.
- [11] P.-M. Zhan, Z.-H. He, Z.-M. Ma, C.-F. Liang, X.-X. Zhang, A.A. Abreham, J.-Y. Shi, Utilization of nano-metakaolin in concrete: A review, Journal of Building Engineering 30 (2020), 101259.
- [12] V.M. Malhotra, High-performance high-volume fly ash concrete, Concr. Int. 24 (7) (2002) 30–34.
- [13] M. Amran, R. Fediuk, G. Murali, S. Avudaiappan, T. Ozbakkaloglu, N. Vatin, M. Karelina, S. Klyuev, A. Gholampour, Fly ash-based eco-efficient concretes: A comprehensive review of the short-term properties, Materials 14 (15) (2021) 4264.
- [14] C.D. Atış, High volume fly ash abrasion resistant concrete, J. Mater. Civ. Eng. 14 (3) (2002) 274–277.
- [15] B. Kumar, G.K. Tike, P.K. Nanda, Evaluation of Properties of High-Volume Fly-Ash Concrete for Pavements, Journal of Materials in Civil Engineering 19 (10) (2007) 906–911.
- [16] S. Izquierdo, J. Diaz, R. Mejia, J. Torres, Blended cement containing fluid catalytic cracking catalyst residue ( FCC): hydration and paste microstructure, Revista Ingeniería de Construcción 28 (2) (2013) 141–154.
- [17] ASTM C618–19, Standard Specification for Coal Fly Ash and Raw or Calcined Natural Pozzolan for Use in Concrete, ASTM International, West Conshohocken, PA, 2019.
- [18] R. Siddique, Performance characteristics of high-volume Class F fly ash concrete, Cem. Concr. Res. 34 (3) (2004) 487–493.
- [19] M. Sumer, Compressive strength and sulfate resistance properties of concretes containing Class F and Class C fly ashes, Constr. Build. Mater. 34 (2012) 531–536.
- [20] S. Aydin, H. Yazıcı, H. Yiğiter, B. Baradan, Sulfuric acid resistance of high-volume fly ash concrete, Build. Environ. 42 (2) (2007) 717–721.
- [21] T. Hemalatha, A. Ramaswamy, A review on fly ash characteristics–Towards promoting high volume utilization in developing sustainable concrete, J. Clean. Prod. 147 (2017) 546–559.
- [22] W. Sarwar, K. Ghafor, A. Mohammed, Regression analysis and Vipulanandan model to quantify the effect of polymers on the plastic and hardened properties with the tensile bonding strength of the cement mortar, Results Mater. 1 (2019) 100011.
- [23] D.M. Cotsovov, M.N. Pavlović, Numerical investigation of concrete subjected to compressive impact loading. Part 2: parametric investigation of factors affecting behaviour at high loading rates, Comput. Struct. 86 (1–2) (2008) 164–180.
- [24] M. Li, H. Hao, Y. Shi, Y. Hao, Specimen shape and size effects on the concrete compressive strength under static and dynamic tests, Constr. Build. Mater. 161 (2018) 84–93.
- [25] D.-C. Feng, Z.-T. Liu, X.-D. Wang, Y. Chen, J.-Q. Chang, D.-F. Wei, Z.-M. Jiang, Machine learning-based compressive strength prediction for concrete: an adaptive boosting approach, Constr. Build. Mater. 230 (2020), 117000.
- [26] A. Ahmad, F. Farooq, K.A. Ostrowski, K. Śliwa-Wieczorek, S. Czarnecki, Application of novel machine learning techniques for predicting the surface chloride concentration in concrete containing waste material, Materials 14 (9) (2021) 2297.
- [27] P. Siyah, P. Jain, M. Kumar, Modelling of impact of water quality on recharging rate of storm water filter system using various kernel function based regression, Modeling Earth Systems and Environment 4 (1) (2018) 61–68.
- [28] W. Mahmood, A. Mohammed, New Vipulanandan pq model for particle size distribution and groutability limits for sandy soils, J. Test. Eval. 48 (5) (2019) 3695–3712.
- [29] W. Qadir, K. Ghafor, A. Mohammed, Evaluation the effect of lime on the plastic and hardened properties of cement mortar and quantified using Vipulanandan model, Open Engineering 9 (1) (2019) 468–480.
- [30] C. Vipulanandan, A. Mohammed, Magnetic field strength and temperature effects on the behavior of oil well cement slurry modified with iron oxide nanoparticles and quantified with vipulanandan models, J. Test. Eval. 48 (6) (2019) 4516–4537.
- [31] J.M. Marangu, Prediction of compressive strength of calcined clay based cement mortars using support vector machine and artificial neural network techniques, Journal of Sustainable Construction Materials and Technologies. 5 (1) (2020) 392–398.
- [32] R. Ali, M. Muayad, A.S. Mohammed, P.G. Asteris, Analysis and prediction of the effect of Nanosilica on the compressive strength of concrete with different mix proportions and specimen sizes using various numerical approaches, Struct. Concr. (2022).

- [33] A.K. Ibrahim, H.Y. Dahir, A.S. Mohammed, H.A. Omar, A.H. Sedo, The effectiveness of surrogate models in predicting the long-term behavior of varying compressive strength ranges of recycled concrete aggregate for a variety of shapes and sizes of specimens, *Archives of Civil and Mechanical Engineering* 23 (1) (2023) 61.
- [34] A. Ahmed, P. Abubakr, A. Salih Mohammed, Efficient models to evaluate the effect of C3S, C2S, C3A, and C4AF contents on the long-term compressive strength of cement paste, *Structures* 47 (2023) 1459–1475.
- [35] Y. Sargam, K. Wang, I.H. Cho, Machine learning based prediction model for thermal conductivity of concrete, *Journal of Building Engineering* 34 (2021), 101956.
- [36] M.I. Shah, M.N. Amin, K. Khan, M.S.K. Niazi, F. Aslam, R. Alyousef, M.F. Javed, A. Mosavi, Performance evaluation of soft computing for modeling the strength properties of waste substitute green concrete, *Sustainability* 13 (5) (2021) 2867.
- [37] Y. Li, F.N.S. Hishamuddin, A.S. Mohammed, D.J. Armaghani, D.V. Ulrich, A. Dehghanbanadaki, A. Azizi, The effects of rock index tests on prediction of tensile strength of granitic samples: a neuro-fuzzy intelligent system, *Sustainability* 13 (19) (2021) 10541.
- [38] H.U. Ahmed, A.S. Mohammed, A.A. Mohammed, R.H. Faraj, T. Xie, Systematic multiscale models to predict the compressive strength of fly ash-based geopolymers concrete at various mixture proportions and curing regimes, *PLoS One* 16 (6) (2021) e0253006.
- [39] R.H. Faraj, A.A. Mohammed, A. Mohammed, K.M. Omer, H.U. Ahmed, Systematic multiscale models to predict the compressive strength of self-compacting concretes modified with nanosilica at different curing ages, *Eng. Comput.* 38 (Suppl 3) (2022) 2365–2388.
- [40] M.L. Wang, V. Ramakrishnan, Evaluation of blended cement, mortar and concrete made from type III cement and kiln dust, *Constr. Build. Mater.* 4 (2) (1990) 78–85.
- [41] B. Rai, S. Kumar, K. Satish, Effect of Fly Ash on Mortar Mixes with Quarry Dust as Fine Aggregate, *Adv. Mater. Sci. Eng.* 2014 (2014) 1–7.
- [42] S.S.M. Ghoneim, S.S. Dessouky, A.A. Elfaraskoury, A.B. Abou Sharaf, Modelling and experimental verification of barrier effect on breakdown voltage of transformer oil using Box-Behnken Design, *Measurement* 147 (2019), 106829.
- [43] W. Emad, A. Salih, R. Kurda, Forecasting the mechanical properties of soilcrete using various simulation approaches, *Structures* 34 (2021) 653–665.
- [44] A.A. Abdalla, A. Salih Mohammed, Theoretical models to evaluate the effect of SiO<sub>2</sub> and CaO contents on the long-term compressive strength of cement mortar modified with cement kiln dust (CKD), *Archives of Civil and Mechanical Engineering* 22 (3) (2022) 105.
- [45] M.H. Akeed, S. Qaidi, H.U. Ahmed, W. Emad, R.H. Faraj, A.S. Mohammed, A. R. Azevedo, Ultra-high-performance fiber-reinforced concrete. Part III: Fresh and hardened properties, *Case Studies Constr. Mater.* 17 (2022) e01265.
- [46] N.S. Piro, A.S. Mohammed, S.M. Hamad, The impact of GGBS and ferrous on the flow of electrical current and compressive strength of concrete, *Constr. Build. Mater.* 349 (2022), 128639.
- [47] A.S. Al-Harthy, R. Taha, F. Al-Maamary, Effect of cement kiln dust (CKD) on mortar and concrete mixtures, *Constr. Build. Mater.* 17 (5) (2003) 353–360.
- [48] A. Abdalla, A.S. Mohammed, Hybrid MARS-, MEP-, and ANN-based prediction for modeling the compressive strength of cement mortar with various sand size and clay mineral metakaolin content, *Archives of Civil and Mechanical Engineering* 22 (4) (2022) 1–16.
- [49] A. Mohammed, S. Rafiq, P. Sihag, R. Kurda, W. Mahmood, Soft computing techniques: systematic multiscale models to predict the compressive strength of HVFA concrete based on mix proportions and curing times, *Journal of Building Engineering*, 33 (2021), 101851.
- [50] I.A. Sharaky, S.S.M. Ghoneim, B.H. Abdel Aziz, M. Emara, Experimental and theoretical study on the compressive strength of the high strength concrete incorporating steel fiber and metakaolin, *Structures* 31 (2021) 57–67.
- [51] D.J. Armaghani, G.D. Hatzigeorgiou, C. Karamani, A. Skentou, I. Zoumpoulaki, P. G. Asteris, Soft computing-based techniques for concrete beams shear strength, *Procedia Struct. Integrity* 17 (2019) 924–933.
- [52] A. Kooshkaki, H. Eskandari-Naddaf, Effect of porosity on predicting compressive and flexural strength of cement mortar containing micro and nano-silica by multi-objective ANN modeling, *Constr. Build. Mater.* 212 (2019) 176–191.
- [53] Asteris, P. G., Apostolopoulou, M., Armaghani, D. J., Cavalieri, L., Chountalas, A. T., Guney, D., ... & Nguyen, H. (2020). On the metaheuristic models for the prediction of cement-metakaolin mortars compressive strength. *1, 1(1)*, 063.
- [54] E.M. Golafshani, A. Behrood, M. Arashpour, Predicting the compressive strength of normal and high-performance concretes using ANN and ANFIS hybridized with Grey Wolf Optimizer, *Constr. Build. Mater.* 232 (2020), 117266.
- [55] H.U. Ahmed, A.A. Abdalla, A.S. Mohammed, A.A. Mohammed, Mathematical modeling techniques to predict the compressive strength of high-strength concrete incorporated metakaolin with multiple mix proportions, *Cleaner Materials* 5 (2022), 100132.
- [56] A. Abdalla, A. Salih, Microstructure and chemical characterizations with soft computing models to evaluate the influence of calcium oxide and silicon dioxide in the fly ash and cement kiln dust on the compressive strength of cement mortar, *Resources, Conservation & Recycling Advances* 15 (2022), 200090.
- [57] D.K.I. Jaf, P.I. Abdulrahman, A.S. Abdulrahman, A.S. Mohammed, Effited soft computing models to evaluate the impact of silicon dioxide (SiO<sub>2</sub>) to calcium oxide (CaO) ratio in fly ash on the compressive strength of concrete, *Journal of Building, Engineering* 106820 (2023).
- [58] H. Song, A. Ahmad, F. Farooq, K.A. Ostrowski, M. Maślak, S. Czarnecki, F. Aslam, Predicting the compressive strength of concrete with fly ash admixture using machine learning algorithms, *Constr. Build. Mater.* 308 (2021), 125021.
- [59] T.R. Naik, S.S. Singh, B.W. Ramme, Effect of Source of Fly Ash on Abrasion Resistance of Concrete, *J. Appl. Sci.* 14 (5) (2002) 417–426.
- [60] L.H. Jiang, V.M. Malhotra, Reduction in water demand of non-air-entrained concrete incorporating large volumes of fly ash, *Cem. Concr. Res.* 30 (11) (2000) 1785–1789.
- [61] N. Bouzoubaa, M. Lachemi, Self-compacting concrete incorporating high volumes of class F fly ash preliminary results, *Cem. Concr. Res.* 31 (3) (2001) 413–420.
- [62] C. Duran Atıç, Strength properties of high-volume fly ash roller compacted and workable concrete, and influence of curing condition, *Cem. Concr. Res.* 35 (6) (2005) 1112–1121.
- [63] C.D. Atis, High-Volume Fly Ash Concrete with High Strength and Low Drying Shrinkage, *J. Mater. Civ. Eng.* 15 (2) (2003) 153–156.
- [64] N. Bouzoubaa, B. Fournier, Optimization of fly ash content in concrete: Part I: non-air-entrained concrete made without superplasticizer, *Cem. Concr. Res.* 33 (7) (2003) 1029–1037.
- [65] G. Baert, A.-M. Poppe, N. De Belie, Strength and durability of high-volume fly ash concrete, *Struct. Concr.* 9 (2) (2008) 101–108.